Received: 31 October 2024 | Accepted: 8 May 2025

DOI: 10.1111/iej.14262

INTERNATIONAL ENDODONTIC JOURNAL | WILEY

ORIGINAL ARTICLE

Exosomal circ_0003057 promotes osteo/odontogenic differentiation of hDPSCs by binding with EIF4A3 through upregulated parental gene ANKH

Bingtao Wang[1] | **Yuanyuan Kong**[1] | **Huixian Dong**[1] | **Feng Lai**[1] | **Zixin Guo**[1] | **Liecong Lin**[1] | **Jingyi Xu**[1] | **Jingkun Zhang**[1] | **Yiguo Jiang**[2] | **Qianzhou Jiang**[1]

[1]Department of Endodontics, Affiliated Stomatology Hospital of Guangzhou Medical University, Guangdong Engineering Research Center of Oral Restoration and Reconstruction, Guangzhou Key Laboratory of Basic and Applied Research of Oral Regenerative Medicine, Guangzhou, Guangdong, China

[2]State Key Laboratory of Respiratory Disease, Institute for Chemical Carcinogenesis, Guangzhou Medical University, Guangzhou, China

Correspondence
Qianzhou Jiang, Department of Endodontics, Affiliated Stomatology Hospital of Guangzhou Medical University, Guangdong Engineering Research Center of Oral Restoration and Reconstruction, Guangzhou Key Laboratory of Basic and Applied Research of Oral Regenerative Medicine, Guangzhou, Guangdong 510182, China.
Email: jqianzhou@126.com

Funding information
National Natural Science Foundation of China, Grant/Award Number: 82270966; Basic and Applied Basic Research Foundation of Guangdong Province, Grant/Award Number: 2022A1515110601; Natural Science Foundation of Guangdong Province, Grant/Award Number: 2024A1515012741

Abstract

Aim: Elucidating the mechanism of osteo/odontogenic differentiation of human dental pulp stem cells (hDPSCs) is crucial for advancing regenerative endodontic procedures (REPs). Circular RNAs (circRNAs) play significant regulatory roles in stem cell differentiation, and exosomes are crucial for intercellular communication. This study investigated the role of exosomal circRNAs in hDPSCs during osteo/odontogenic differentiation using in vitro and in vivo evidence.

Materials and Methods: We isolated hDPSCs from dental pulp tissues of healthy immature permanent teeth. CircRNA microarray analysis was used to identify differentially expressed circRNAs. Exosomes were extracted from hDPSCs using ultracentrifugation, and circRNA content was detected. Functional validation of exosomal circRNAs was performed using siRNA/overexpression plasmids and subcutaneous transplantation in to nude mice. The biological effects of circ_0003057, EIF4A3 and ANKH were determined using real-time quantitative polymerase chain reaction (qRT-PCR), western blotting (WB), alkaline phosphatase (ALP) staining and activity, alizarin red staining (ARS), quantification and immunofluorescence staining. EIF4A3 was identified as a potential binding protein (RBP) for circ_0003057 in the database, and this binding relationship was confirmed using RNA pull-down and RIP assays. qRT-PCR and WB were performed to determine whether the host gene ANKH of circ_0003057 was activated.

Results: circ_0003057 expression was increased during osteo/odontogenic differentiation of hDPSCs, whereas circ_0003057 downregulation suppressed this process. EIF4A3 was confirmed to be a binding protein of circ_0003057 and was upregulated during osteo/odontogenic differentiation of hDPSCs. Further investigation revealed that circ_0003057 upregulation during osteo/odontogenic differentiation led to the upregulation of its parental gene, ANKH. Co-transfection experiments confirmed that circ_0003057 upregulated ANKH, promoting osteo/odontogenic differentiation of hDPSCs.

Bingtao Wang and Yuanyuan Kong contributed equally to this work.

Conclusions: This study demonstrates that exosomal circ_0003057 promotes osteo/odontogenic differentiation of hDPSCs by interacting with EIF4A3 and upregulating ANKH, providing new insights into the molecular mechanisms underlying this process and its potential applications in regenerative endodontics.

KEYWORDS

circRNA, exosome, stem cell

INTRODUCTION

Regenerative endodontic procedures (REPs) have become an important approach for treating young permanent teeth with pulpal and periapical diseases (Høiby et al., 2011). However, existing treatments are unable to reconstruct a fully functional pulp-dentine complex. Stem cells derived from teeth can differentiate into various functional cells to generate dental pulp-dentine complex-like structures (Huang et al., 2009). Human dental pulp stem cells (hDPSCs) exhibit high proliferation, self-renewal and multi-lineage differentiation potential. Osteo/odontogenic differentiation refers to the simultaneous activation of both odontogenic (dentine-forming) and osteogenic (bone-forming) molecular programmes in hDPSCs under in vitro mineralization-inducing conditions. This hybrid state, enabled by their shared neural crest origin and overlapping regulatory pathways, with in vitro expression of osteogenic markers and in vivo capacity to form dentine-like structures, reflecting hDPSCs plasticity for regenerative strategies targeting dentine and bone (Batouli et al., 2003; Huang et al., 2009). These cells differentiate into odontoblasts and contribute to dentine-pulp complex (DPC) formation in vivo (Nuti et al., 2016). Although mechanisms on how stem cells derived from teeth differentiate into odontoblasts have been investigated, the process has not been well clarified (Tye et al., 2015).

During the osteo/odontogenic differentiation of hDPSCs, the surrounding extracellular matrix components change (Liu et al., 2007). Studies have found that using the extracellular matrix of dental pulp tissue can effectively promote the proliferation and differentiation of hDPSCs (Li et al., 2020). Moreover, research has highlighted the significant role of exosomes in this process (Nawaz et al., 2018). Exosomes are extracellular vesicles ranging from 30 to 150 nm in diameter (Doyle & Wang, 2019). Using exosomes from DPSCs can alleviate bone resorption and promote bone healing in the alveolar bone during periodontitis (Shen et al., 2020). Another study promoted the mineralization of hDPSCs by releasing odontogenic exosomes from mDPSCs via a biodegradable carrier aggregate (Swanson et al., 2020). The above studies demonstrate that exosomes from DPSCs can effectively promote cell stemness, viability and proliferative capacity, enhancing the osteo/odontogenic differentiation of hDPSCs. In the field of pulp regeneration, exosomes can be used as an alternative to live-cell therapy to activate the differentiation of residual pulp stem cells and regulate the inflammatory microenvironment by slow release of active molecules loaded on biomaterial scaffolds, thus promoting the regeneration of the pulp-dentine complex (Villani et al., 2024). However, the specific mechanism by which exosomes promote osteo/odontogenic differentiation of hDPSCs remains unknown.

Despite these advances, the molecular mechanisms by which exosomal circRNAs regulate osteo/odontogenic differentiation of hDPSCs remain poorly understood. Exosomes contain a specific composition of functional messenger RNAs (mRNAs), microRNAs (miRNAs), long noncoding RNAs (lncRNAs), circular RNAs (circRNAs) and proteins that play important roles in cell-to-cell communication by transferring messages (Li, Li, et al., 2018; Liu et al., 2019; Qu et al., 2016). CircRNAs are indispensable in post-transcriptional regulation. (Hansen et al., 2013; Liu et al., 2017) CircRNAs are a class of ncRNAs produced by back splicing, and their loop structure makes them more stable (Kristensen et al., 2019). CircRNAs participate in the process of transcriptional and post-translational regulations of gene expression (Chen et al., 2017). In addition, they play important roles in osteoblast differentiation and odontogenic differentiation (Li, Zheng, et al., 2018; Liu et al., 2023; Zhang et al., 2019).

Exosomes carry diverse RNA cargoes, including circular RNAs (circRNAs)—stable, noncoding RNAs formed by back splicing. CircRNAs regulate gene expression through multiple mechanisms, including acting as miRNA sponges, modulating parental gene transcription, binding to RNA-binding proteins (RBPs) and even encoding peptides (Huang et al., 2020; Panda, 2018; Wan et al., 2016; Zheng et al., 2019). Many circRNAs were predicted to interact with RNA binding proteins (RBPs). (Hentze & Preiss, 2013) Some RBPs, such as Argonaute and MBL, can bind to circRNAs (Ashwal-Fluss et al., 2014). By forming complexes with circRNAs, RBPs affect circRNA function by influencing RNA maturation, translocation, localization and translation (Huang et al., 2020). The circular RNA in cervical cancer studies, circ-PABPN1, has been reported to bind to HuR inhibited the expression of

the parental gene PABPN1 (Abdelmohsen et al., 2017). Whilst several circRNAs (e.g. circIGSF11, circ_0026827) have been implicated in osteo/odontogenic differentiation via miRNA sponging, the role of circRNA–protein interactions in this process remains underexplored (Ju et al., 2023). However, other potential mechanisms of circRNA's role in the osteo/odontogenic differentiation of hDPSCs remain to be elucidated.

Using circRNA microarray analysis, we identified circ_0003057 as a highly upregulated circRNA during hDPSCs osteo/odontogenic differentiation, particularly in exosomes. This study aims to elucidate how circ_0003057 interacts with its parental gene ANKH and the RNA-binding protein EIF4A3 to regulate osteo/odontogenic differentiation. Our data provide new insights into the molecular mechanisms by which exosomes act on osteo/odontogenic differentiation of hDPSCs and their potential application in regenerative endodontics.

MATERIALS AND METHODS

The manuscript of this laboratory study has been written according to Preferred Reporting Items for Laboratory studies in Endodontology (PRILE) 2021 guidelines (Nagendrababu et al., 2021).

Isolation and culture of hDPSCs

The Ethics Committee of the Hospital of Stomatology of Guangzhou Medical University approved this study (No. JCYJ2024029). All the DPSCs used in our experiments were derived from human patients. Cells were isolated from third molars or orthodontically extracted teeth free from caries or periodontal disease. These teeth were obtained from the Hospital of Stomatology of Guangzhou Medical University with informed consent from eight patients aged 16–24 years. The extraction process involved clipping the dental pulp with scissors, thoroughly rinsing it multiple times with phosphate-buffered saline (PBS, C10010500BT, Gibco) supplemented with penicillin–streptomycin and digesting with 1 mg/mL Type I collagenase (v900692, VETEC) for 40 min at 37°C. The dental pulp fragments were then cultured in a medium containing 20% FBS at 37°C and 5% CO_2 for 10 days to derive primary hDPSCs. These extracted hDPSCs were subsequently cultured in alpha-modified Minimum Essential Medium (α-MEM; C11995500BT; Gibco, Waltham, MA, USA), supplemented with 10% foetal bovine serum (FBS; 10099141, Gibco) and 1% penicillin–streptomycin (SV30010; HyClone, South Logan, UT, USA), in a 37°C incubator (Binder, Baruth, Germany) with 5% CO_2. Upon reaching 80% cell density, the cells were treated with 0.25% trypsin–EDTA (10525E16; Gibco) and reseeded in multi-well plates for further experiments. hDPSCs between passages three and six were used in this study.

For osteo/odontogenic differentiation, hDPSCs were cultured in 6-well plates at a density of 1×10^5 cells/well. The osteo/odontogenic differentiation culturing medium contained α-MEM with 10% FBS, 50 mg·mL^{-1} ascorbic acid, 10 mM sodium β-glycerophosphate and 10 nm dexamethasone (Sigma Aldrich, St. Louis, MO, USA).

CircRNA microarray

After osteo/odontogenic differentiation of hDPSCs for 0, 3 and 7 days, total RNA was isolated from the cultured cells. Total RNA was isolated using the TRIzol reagent (Invitrogen, Carlsbad, MA, USA) according to the manufacturer's instructions. Subsequently, a circRNA microarray analysis (Huada Bio-tech, Shenzhen, China) was conducted using samples from osteo/odontogenic induction at 0, 3 and 7 days. Differentially expressed circRNAs were identified based on fold change (>2) and $p<0.05$.

Exosome isolation, identification and internalization of exosomes

hDPSCs were cultured in osteo/odontogenic differentiation culture medium for osteo/odontogenic differentiation for 0, 7 and 14 days and then cultured in FBS-free medium for 48 h. In brief, the culture supernatant was collected and concentrated using centrifugation in the concentrator tube (20 min, 2000 g·s^{-1}), and the exosomes were obtained using separation in an ultracentrifuge (100 000 g·s^{-1}, 17 h); the exosomes were then resuspended in PBS and stored at −80°C until use. The size of the exosomes was determined using a nanoparticle tracking analysis (NTA) instrument (ZetaView, Kunzelsau, Germany). The morphology of the exosomes was observed using a transmission electron microscope (TEM; StarJoy, Guangzhou, Japan). The surface markers TSG101, CD63 and Calnexin in the exosomes were analysed using western blotting.

Isolated exosomes were labelled with PKH26 red fluorescence dye (Umibio, UR52302, Shanghai, China) and incubated for 30 min at 37°C. Subsequently, hDPSCs were co-cultured with labelled exosomes for 12 h at 37°C. The nuclei of the hDPSC cells were stained with DAPI (blue), and the cytoskeleton of the hDPSCs was stained with phalloidin (green). Subsequently, the internalization of exosomes by hDPSCs was measured using laser scanning confocal microscopy (Leica, Buffalo Grove, IL, USA).

Multilineage differentiation potential of hDPSCs

The induction of mineralization of hDPSCs is shown above. For ARS staining, hDPSCs were fixed with 4% paraformaldehyde for 10 min and were stained with Alizarin Red solution (Beyotime) in mineral nodules for 10 min and then visualized with a stereomicroscope.

The induction medium for chondrogenic differentiation was prepared and configured according to the manufacturer's instructions (Oricell, Guangdong, China). Then, 3×10^6 hDPSCs were seeded into 15-mL centrifuge tubes containing 0.5 mL of induction medium. Subsequently, the tubes were placed in an incubator set at 37°C, and the medium was refreshed every 3 days. When the diameter of the chondrospheres reached 1–1.5 mm, paraffin sections were prepared and stained with Alcian Blue 8GX Solution.

A stem cell adipogenic differentiation kit (Starfish cos9X Bio, Jiangsu, China) was used according to the manufacturer's instructions. A total of 1×10^5 human dental pulp stem cells (hDPSCs) were seeded into 12-well plates. The cells were first cultured in the induction medium for 3 days, followed by 1 day of culture in the maintenance medium. The cells were cultured for 21 days, and the medium was changed at the frequency described above. Finally, the cells were stained with Oil Red O and observed under a light microscope.

Flow cytometry assay

Cell surface antigen identification of hDPSCs cultured in generation 4 was performed using flow cytometry. Cells (1×10^7) were digested with 0.25% trypsin, incubated for 45 min in PBS and incubated with anti-CD34 (Invitrogen) CD19 (Biolegend, San Diego, CA, USA), CD14 (Invitrogen), anti-HLA-DR (Biolegend), CD90 (Biolegend), CD73 (Biolegend), CD105 (Invitrogen) and CD45 (TONBO, San Diego, CA, USA). Data were analysed using a FACSCalibur flow cytometer (Novocyte 3005; Agilent, Santa Clara, CA, USA).

RNA preparation and quantitative reverse transcriptase polymerase chain reaction (qRT-PCR) analysis

Total RNA was isolated from cultured cells using a Total RNA Kit (B0004D; EZBioscience, Roseville, MN, USA) according to the manufacturer's protocol. Additionally, RNA from the nuclear and cytoplasmic compartments was separated using the FastPure Cytoplasmic and Nuclear RNA Purification Kit (Ecotop Scientific, Xiamen, China) according to the manufacturer's protocol. The reverse transcriptase reaction was performed using the Evo M-MLV reverse transcriptase reagent premix (AG11706; Accurate Biology, Hunan, China) for circRNA and mRNA. RNA expression was measured using quantitative real-time PCR analysis with the CFX Connect Real-Time System (Bio-Rad, Hercules, CA, USA) and SYBR Green Reagent (Q711-02; Vazyme, Nanjing, China). GAPDH was used as a reference gene control for circRNA and mRNA levels of total RNA and RNA in the cytoplasm. U6 was used as the reference gene control for nuclear cRNA. Primers were synthesized by IGE Biotechnology (GuangZhou, China), and all sequences are available in Supplementary file: Table S1. The $2^{-\Delta\Delta CT}$ method was used to calculate relative expression levels of mRNA and circRNA.

Western blot analysis

Cells were lysed using pre-cooled RIPA cracking buffer (ST507; Beyotime, Shanghai, China) containing 1% PMSF (P0013B; Beyotime). After centrifuging at 12000 rpm for 10 min at 4°C, total protein was collected from the lytic cells. Proteins were quantified using a BCA kit (P0012; Beyotime), according to the manufacturer's instructions. Equal amounts (20 μg) of protein were loaded onto a 10% sodium dodecyl sulphate-polyacrylamide gel. The proteins were separated via electrophoresis and transferred onto PVDF membranes (IPVH20200; Millipore, Billerica, MA, USA). The membrane was blocked for 1 h at 25°C and incubated at 4°C overnight with primary antibodies: GAPDH (1:1000; Abcam, Cambridge, United Kingdom), DSPP (1:1000; Abcam), DMP-1 (1:1000; Biodragon, Suzhou, China), ANKH (1:1000; ABclonal, Wuhan, China) and EIF4A3 (1:1000; Abcam). After washing with Tris-buffered saline thrice for 5 min each, the membranes were incubated with secondary antibodies labelled with horseradish peroxidase (1:10000; SAB, USA) at room temperature for 1 h and the bands were developed by semi-quantitative analysis using optical density scanning. Target bands were quantified using ImageJ software and normalized to GAPDH.

ARS and ALP staining

For ARS staining, hDPSCs were fixed with 4% paraformaldehyde for 10 min, and the mineral nodules were stained with Alizarin Red solution (Beyotime) for 10 min using a stereoscopic microscope. After alizarin red staining, the 0.1 g·mL^{-1} solution of cetylpyridinium chloride was configured to dissolve the mineralized nodules at 37°C for 12 h.

Absorbance was measured at 562 nm using a microplate reader for semi-quantitative analysis.

For ALP staining, 7 days after hDPSCs osteo/odontogenic induction, cells from each group were fixed with 4% paraformaldehyde for 10 min. The cells were then stained using the CIP/NBT Alkaline Phosphatase Colour Development Kit (Beyotime) and observed under a stereoscopic microscope. ALP activity was quantified using an Alkaline Phosphatase Assay Kit (Beyotime) by detecting the cell lysates according to the manufacturer's instructions.

Cell transfection and infection

Small interfering RNA plasmid targeting (circ_0003057, EIF4A3), short hairpin RNA (ANKH), overexpression plasmid pcDNA3.1(circ_0003057, ANKH, EIF4A3) and control (NC) were synthesized by GenePharma (Hangzhou, China). When the fusion rate of hDPSCs was 70%–80%, transfection was performed using lipo3000 (Invitrogen), according to the manufacturer's instructions. After 48 h of transfection, total RNA was collected and the mRNA expression level was determined using qRT-PCR to verify the transfection efficiency. After 48 h of transfection, the cells were cultured in an osteo/odontogenic medium for osteo/odontogenic cell differentiation.

RNase R digestion assays

For the RNase R assay, total RNA in hDPSCs was incubated with or without RNase R for 30 min at 37°C, respectively. After treatment with RNase R, the expression levels of GAPDH, circ_0003057 and the parental gene ANKH were detected using qRT-PCR.

Fluorescence in situ hybridization (FISH)

An oligonucleotide probe for circ_0003057 was designed and synthesized RiboBio (Guangzhou, China). FISH assays were performed using the Ribo™ Fluorescence in Situ Hybridization (FISH) Kit (Beyotime) as described in the reagent manufacturer's protocol. Images were captured using a confocal laser scanning microscope (Leica, Buffalo Grove, IL, USA).

RNA pull-down and RIP

RNA pull-down analysis was performed using an RNA pull-down kit (Bes5102, Bersinbio, GuangZhou, China) according to the manufacturer's protocol. Biotin-labelled probes targeting the junction site of flanking sequences of circ_0003057 were synthesized by Sangong Biotech (Shanghai, China). The sequences are available in Supplementary file: Table S2. Cell lysates were incubated with a biotin-labelled probe, and the protein samples were further characterized using western blotting. RNA binding protein immunoprecipitation (RIP) assays were performed using the RNA Binding Protein Immunoprecipitation Kit (Millipore) according to the manufacturer's protocol. Co-precipitated RNA expression levels were detected using qRT-PCR with circ_0003057 specific primers.

Animal studies

The Laboratory Animal Ethics Committee of Guangdong Ruiye Testing Co Ltd. approved this animal study. The animals were cared for in accordance with the guidelines established by the Laboratory Animal Ethics Committee of Guangdong Ruiye Testing Co Ltd. All experimental procedures were performed on 6-week-old nude mice ($n = 6$ per group) under general anaesthesia. First, 100 μg of Exo and 1×10^6 hDPSCs mixed with Cellmatrix Type I (Cellmatrix, Osaka, Japan) were incorporated into 3 mm thick human dental fragments. These were subsequently transplanted subcutaneously into the backs of mice. Each mouse received four sets of dental fragments corresponding to the following groups: (1) blank control, (2) hDPSCs, (3) EXO 0d + hDPSCs and (4) EXO 7d + hDPSCs. The animals were provided ad libitum access to food and water and were euthanized 8 weeks after implantation.

Following tissue decalcification, samples were cut into 5-μm-thick sections. These sections were processed with graded alcohol and stained using haematoxylin and eosin (HE) and Masson's trichrome. The stained sections were then sealed with neutral gum and examined under a light microscope to observe histological changes.

Statistical analysis

Statistical analyses were performed using GraphPad Prism version 9.0. Data are presented as mean ± standard deviation (SD). Statistical differences between two groups were evaluated using a two-tailed independent Student's t-test. One-way analysis of variance (ANOVA) was used for comparisons amongst three or more groups. Post-hoc comparisons following ANOVA were performed using Tukey's test. $p < 0.05$ was considered statistically significant.

RESULTS

Circ_0003057 expression increases in hDPSCs during the osteo/odontogenic differentiation

The primary hDPSCs were successfully isolated (Figure S1a). Flow cytometry analysis revealed that hDPSCs highly expressed CD73 (98%), CD90 (98.38%) and CD105 (97.34%) but were negative for CD34 (0.29%), CD19 (0.07%) and HLA-DR (0.11%) (Figure S1e). Alizarin red staining demonstrated that hDPSCs formed numerous mineralized nodules, indicating their capacity to differentiate into osteoblasts (Figure S1b). Oil red staining showed that hDPSCs formed abundant lipid droplets, indicating their ability to differentiate into adipocytes (Figure S1c). Alcian blue staining revealed that the hDPSCs formed cartilage nodules, demonstrating their potential to differentiate into chondrocytes (Figure S1d). We extracted hDPSCs as mesenchymal stem cells with good multidirectional differentiation ability.

To explore the potential involvement of circRNAs in osteo/odontogenic differentiation, we identified the circRNAs differentially expressed in hDPSCs during osteo/odontogenic induction using circRNA sequencing (RNA-seq). Through RNA-seq analysis, we identified 3963 upregulated circRNAs after osteo/odontogenic differentiation for 3 days and 4844 upregulated circRNAs after osteo/odontogenic differentiation for 7 days compared to the normal group (Figure 1a). The top 50 circRNAs with the most significant upregulation on days 3 and 7 excluded the circRNAs that could not be paired with circBase, for which it was difficult to design primers. Ultimately, 13 circRNAs were chosen as candidate circRNAs for this study and validated via qRT-PCR. Circ_0073806 and circ_0003057 were the most significantly upregulated genes (Figure 1b). Circ_0003057 corresponded to exo_circ_59116, and circ_0073806 was not found in the exoRBase database. After analysing and comparing these results, circ_0003057 was selected for further analysis (Figure 1c).

According to the analysis of databases such as circBase, circBank and NCBI, circ_0003057 was formed by the 3′-8′ splice site of the mRNA exon 3′-8′ of the human ankyrin motif (ANKH) originating from the gene located on chr5:14741935–14 758 707, and its length was 698 nt. The back-splicing junction site of circ_0003057 was identified using Sanger sequencing (Figure 1e). To further assess the circular characteristics of circ_0003057, we performed an RNase R-resistance assay, which showed that circ_0003057 was hardly digested, whereas its linear parental gene, ANKH, was markedly degraded (Figure 1d). To explore the cellular distribution of circ_0003057, we performed a nucleoplasmic segregation assay, which showed that circ_0003057 was predominantly localized in the cytoplasm (Figure 1f). FISH analysis also showed that circ_0003057 was mainly expressed in the cytoplasm (Figure 1g). These results demonstrated that circ_0003057 has a stable circular structure and is mainly located in the cytoplasm of hDPSCs.

Exosomal circ_0003057 promotes osteo/odontogenic differentiation of hDPSCs

There was evidence that intercellular communication, proliferation and metabolism could be realized through the transfer of circRNA carried by exosomes to recipient cells (Deng et al., 2023). To investigate whether exosomal circRNAs influenced the function of osteo/odontogenic differentiation, we extracted the exosomes from early, middle and late stages of hDPSCs osteo/odontogenic differentiation on days 0, 7 and 14, and named them EXO 0d, EXO 7d and EXO 14d, respectively. TEM revealed that the morphology of the extracted exosomes was cup-plate-shaped (Figure 2a). The particle size of the exosomes was measured using a particle size analyser (NTA) in the range of 30–150 nm, with an average particle size of 80.74 nm (Figure 2b). Western blotting showed positive expression of the specific marker proteins CD63 and TSG101 and negative expression of the negative protein Calnexin in the extracted exosomes (Figure 2c). These results are consistent with the characteristics of exosomes. To verify the biological activity of exosomes, we co-cultured them with hDPSCs for 12 h. Exosomes were labelled with PKH26 (red), the cytoskeleton of the cells was labelled with phalloidin (green) and the nuclei were labelled with DAPI (blue). The exosomes were observed using fluorescence confocal microscopy, and the red markers were observed around the blue marker compared with those of the control group (Figure 2d), which indicated that hDPSCs could take up exosomes.

RNA extracted from the EXO 0d, EXO 7d, and EXO 14d groups was analysed using qRT-PCR. RT-qPCR analysis revealed that the EXO 7d group exhibited the highest circ_0003057 expression level (Figure 2e). We co-cultured three different exosomes with hDPSCs and induced osteo/odontogenic differentiation. In the qRT-PCR analysis, compared with the other groups, the highest expression levels of the osteo/odontogenic-associated genes ALP, RUNX-2, OCN, BSP, DSPP and DMP-1 were found in the EXO 7d group (Figure 2f). Western blotting showed the same trend in the expression levels of DMP-1 and DSPP proteins (Figure 2g).

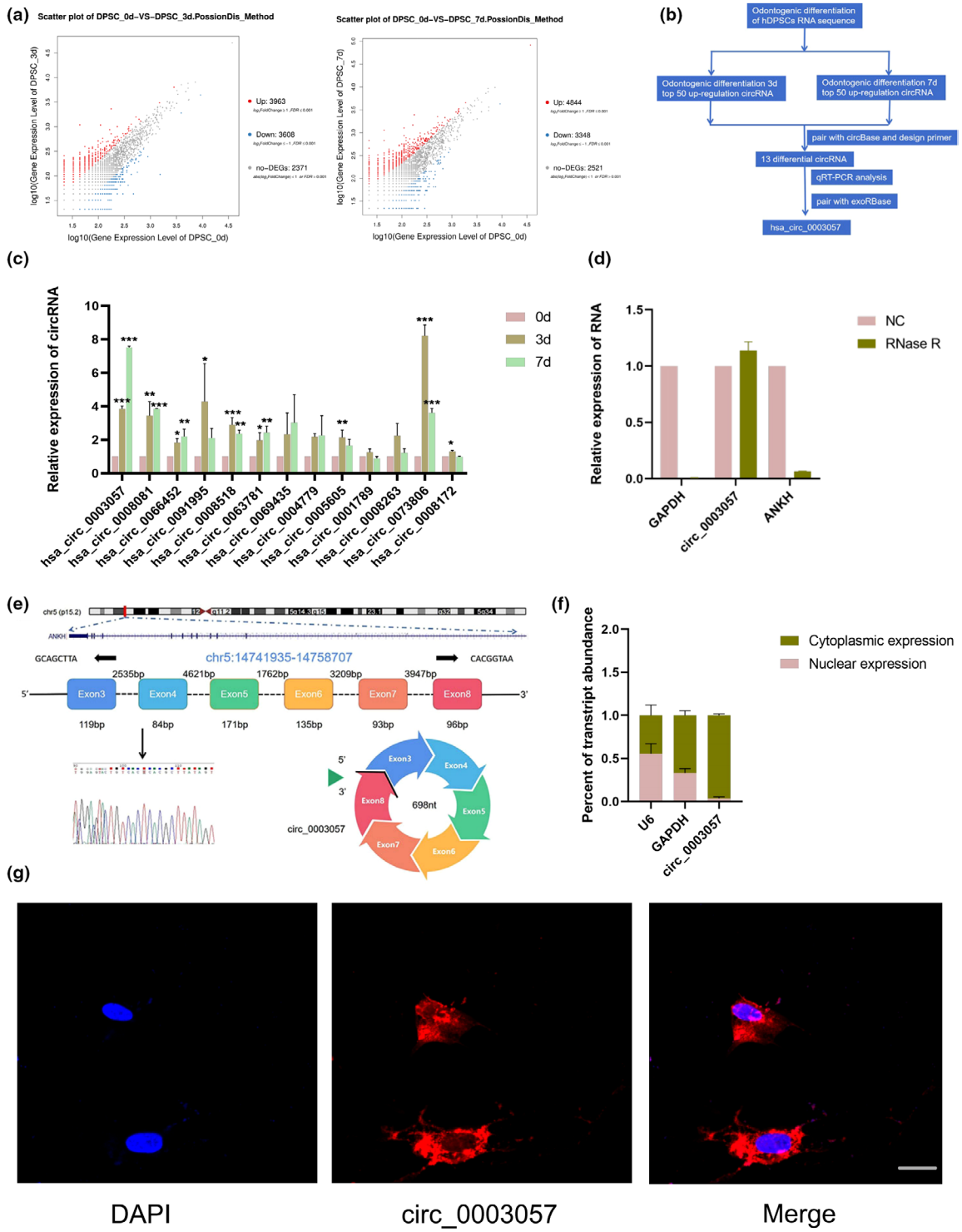

FIGURE 1 Circ_0003057 expression increases in hDPSCs during the osteo/odontogenic differentiation. (a) Scatter plots depicting the distribution of all expressed circRNAs. (b) Flowchart outlining the screening process for target circRNAs. (c) Relative expression levels of 13 upregulated circRNAs screened using qRT-PCR assay. (d) qRT-PCR to detect the expression levels of GAPDH, circ_0003057 and parental genes ANKH after digestion treatment with RNase R in hDPSCs. (e) The qRT-PCR product of the reverse splice site of circ_0003057 was determined by Sanger sequencing. (f) qRT-PCR experiments of nuclear (Nuc) and cytoplasmic (Cyt) isolation assays. (g) FISH analysis. circ_0003057 probe was labelled with CyC3 (red) and nuclei were labelled with DAPI staining (blue). Scale bar: 25 μm. Quantitative data from three independent experiments are shown as the mean ± SD (error bars). $n = 3$ biologically independent samples. *$p < 0.05$, **$p < 0.01$ and ***$p < 0.001$. $n = 3$ biologically independent samples.

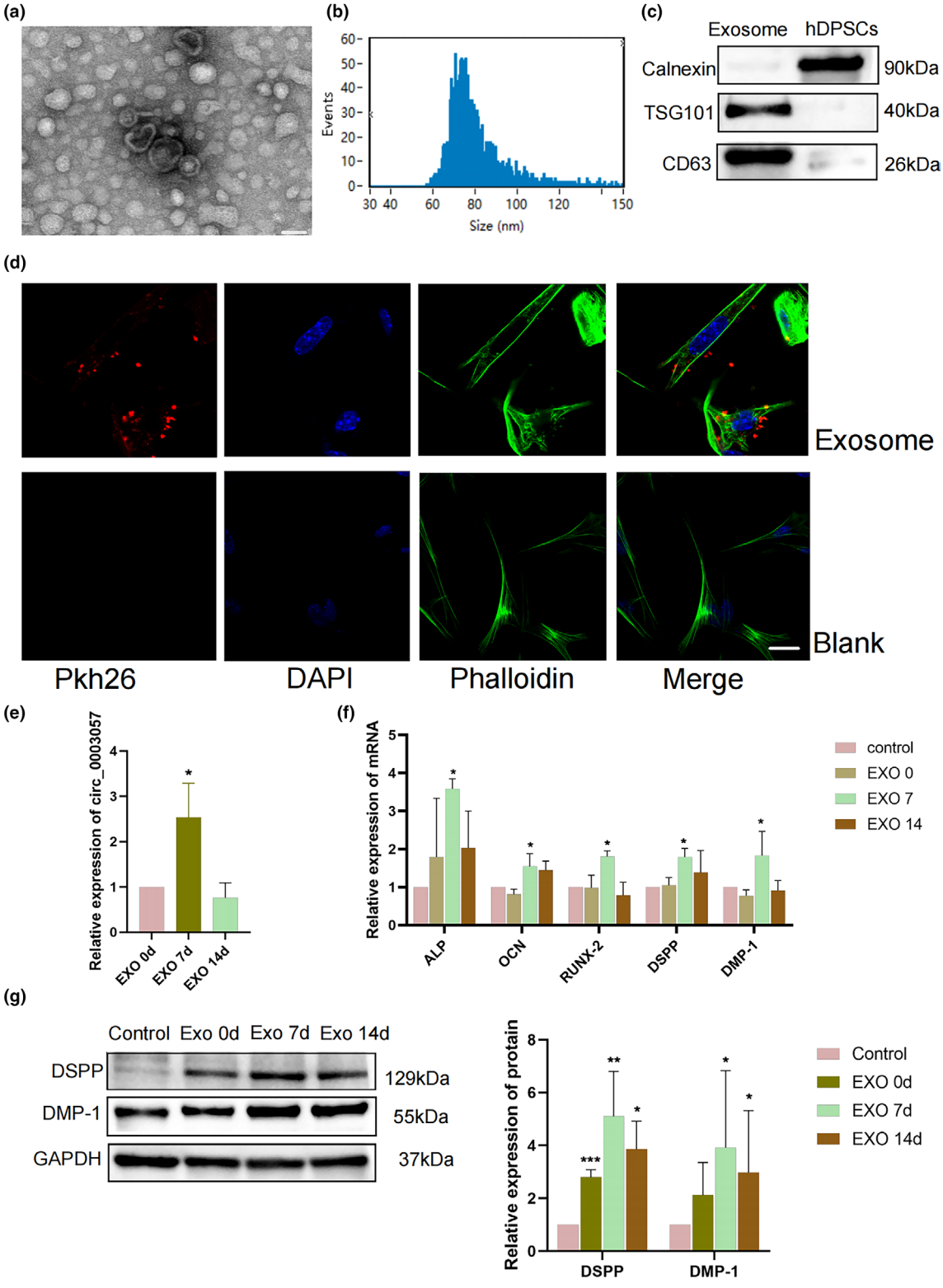

FIGURE 2 Exosome circ_0003057 promotes osteo/odontogenic differentiation of hDPSCs. (a) Transmission electron microscopy analysis of exosomes. Scale bar: 100nm. (b) NTA analysis of exosomes. **(c)** Western blot analysis of exosome. (d) Pkh26-labelled exosomes (red), cell nuclei stained with DAPI (blue) and cytoskeleton of cell stained with Phalloidin (green). Scale bar: 25 μm. (e) qRT-PCR analysis of the level of circ_0003057 in exosome. (f) qRT-PCR analysis expression of ALP, OCN, RUNX-2, DSPP and DMP-1 after co-culture with exosomes. (g) Western blot and semi-quantitative analysis of circ_0003057 protein expression levels osteo/odontogenic-associated markers of DSPP and DMP-1 after co-culture with exosomes. (h) Alkaline phosphatase and quantitative analysis after co-culture with exosomes. Scale bar: 1 mm. (i) Alizarin red and semi-quantitative analysis after co-culture with exosomes. Scale bar: 1 *mm*. *$p < 0.05$, **$p < 0.01$ and ***$p < 0.001$. Quantitative data from three independent experiments are shown as the mean ± SD (error bars). *$p < 0.05$, **$p < 0.01$ and ***$p < 0.001$. $n = 3$ biologically independent samples.

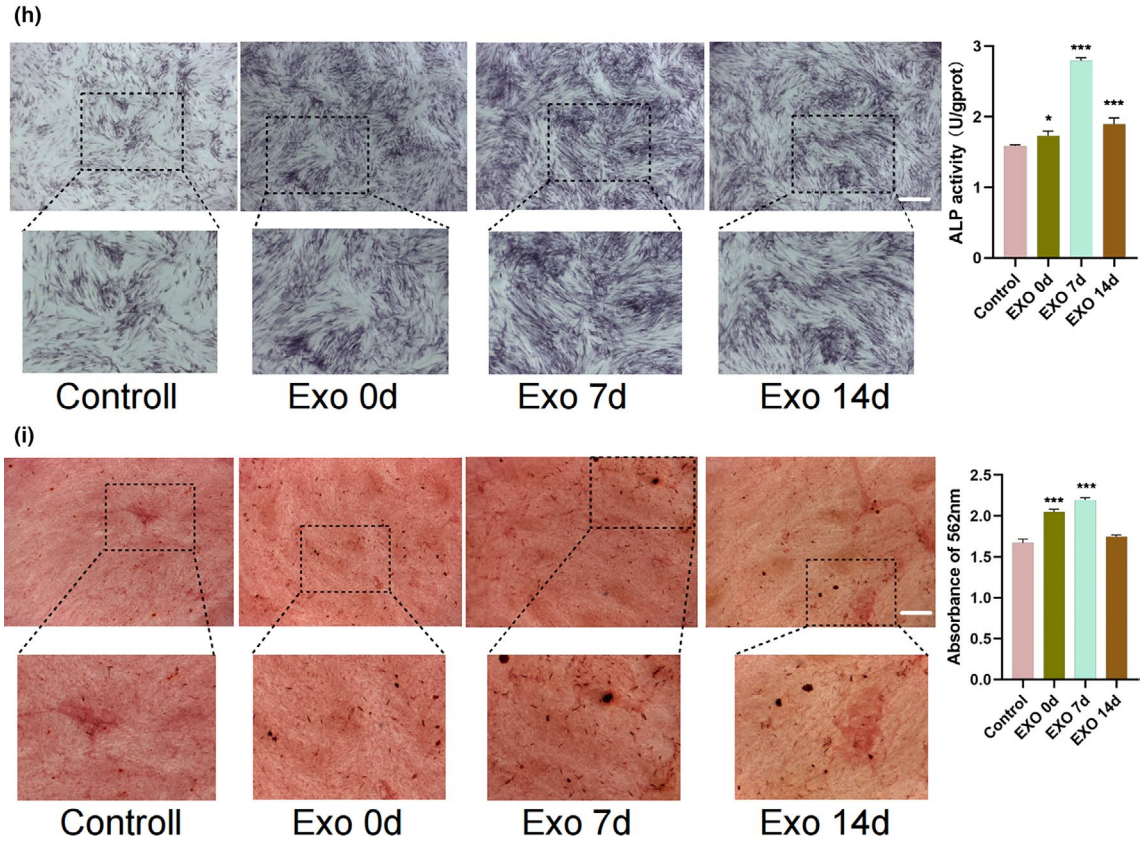

FIGURE 2 (Continued)

Chromogenic treatment with ALP showed that the ALP activity was significantly higher in the EXO 7d group than in the other groups (Figure 2h). Alizarin red staining and semi-quantitative results showed that the EXO 7d group exhibited more highly mineralized nodules (Figure 2i). These results suggest that exosomes deliver circ_0003057 to hDPSCs, promoting osteo/odontogenic differentiation of hDPSCs.

Circ_0003057 promotes osteo/odontogenic differentiation of hDPSCs

To investigate the molecular mechanism of circ_0003057 in osteo/odontogenic differentiation of hDPSCs, we designed two siRNAs targeting the circ_0003057 back-splicing junction site and detected the efficiency of transfection by qRT-PCR. Both si-circ1 and si-circ2 reduced circ_0003057 expression, with the inhibitory effect of si-circ2 being more pronounced (Figure 3a). The qRT-PCR assay revealed a decrease in the expression levels of osteo/odontogenic-related marker genes ALP, OCN, RUNX-2, BSP, DSPP and DMP-1 after interference of circ_0003057 and that the inhibitory effect of the si-circ2 group was more obvious (Figure 3b). The protein expression levels showed the same trend. Western blotting showed that as the expression of circ_0003057 decreased, the expression levels of DSPP and DMP-1 also decreased (Figure 3c). ALP activity was significantly inhibited in the si-circ1 and si-circ2 groups compared to that in the control group (Figure 3d). Alizarin red staining showed that the number of mineralized nodules and the degree of mineralization in the si-circ1 and si-circ2 groups after 14-day induction culture were significantly lower than those in the control group (Figure 3e).

To improve the expression of circ_0003057, we designed an overexpression plasmid for circ_0003057 and successfully transfected it into hDPSCs (Figure 3f). The mRNA expression levels of ALP, RUNX-2, OCN, BSP, DSPP and DMP-1 significantly increased after transfection with the overexpression plasmid (Figure 3g). Western blotting showed the same trend, and the expression levels of DSPP and DMP-1 were increased in the overexpression group (Figure 3h). ALP activity in the overexpression group was significantly higher than that in the negative control group (Figure 3i). Alizarin red staining showed that the overexpression group formed significantly more mineralized nodules, and the degree of mineralization was significantly greater than that in the negative control group (Figure 3j). These results suggest that circ_0003057 promotes osteo/odontogenic differentiation of hDPSCs.

Upregulated expression of ANKH promotes osteo/odontogenic differentiation of hDPSCs

Previous studies have shown that circRNAs regulate cellular functions via parent-dependent mechanisms (Wan et al., 2016). To research the function of circ_0003057 parental gene ANKH with respect to osteo/odontogenic differentiation, we designed corresponding over expression plasmids and short hairpin RNAs for ANKH sequences and tested their corresponding expression efficiencies (Figure 4a,c). After transfection with the

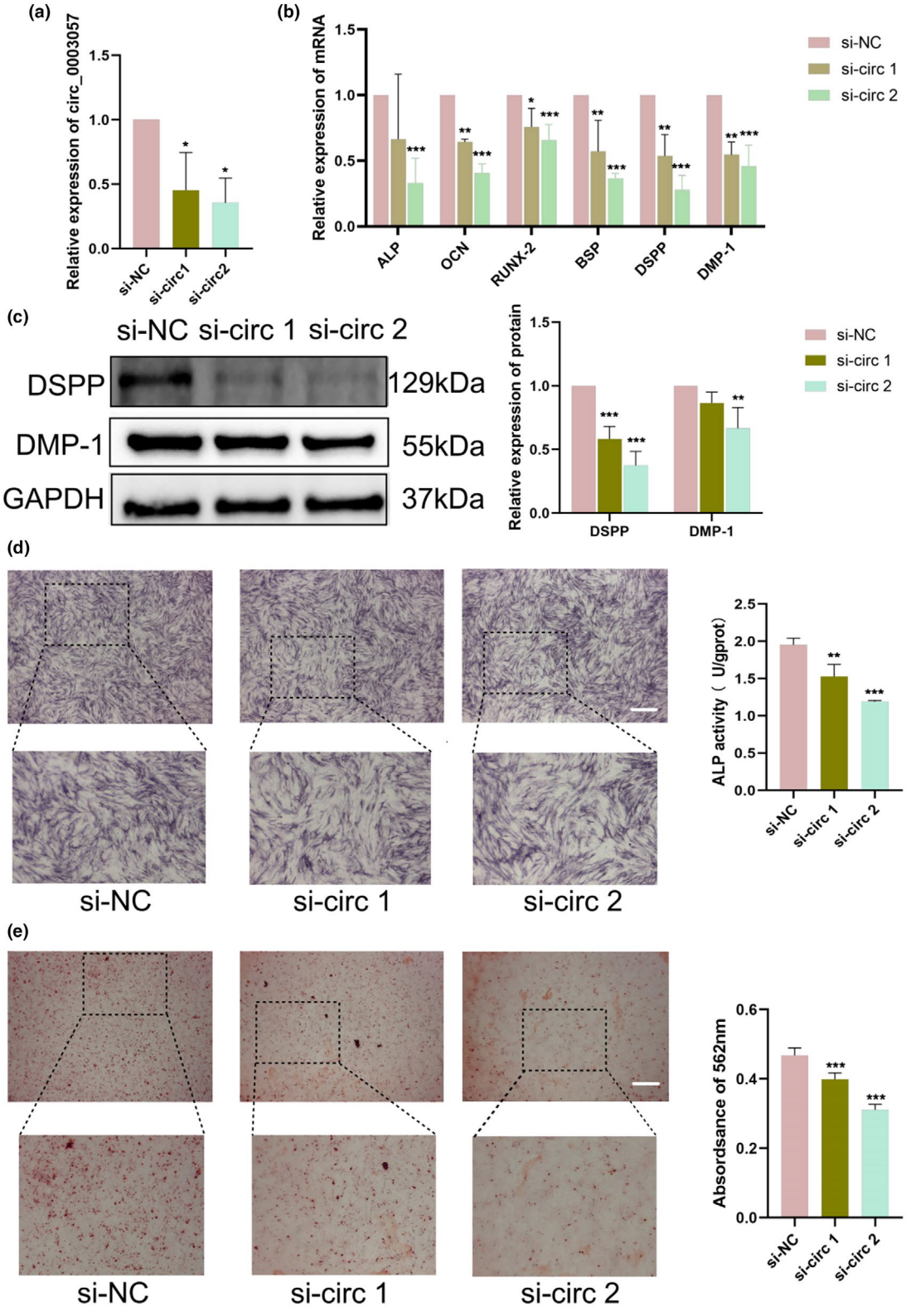

FIGURE 3 Circ_0003057 promotes osteo/odontogenic differentiation of hDPSCs (a) qRT-PCR analysis of the transfection efficiency of siRNA. (b) qRT-PCR analysis of the expression of ALP, OCN, RUNX-2, BSP, DSPP and DMP-1 after siRNA of circ_0003057 transfection. (c) Western blot and semi-quantitative analysis of DSPP, DMP-1 proteins in hDPSCs after siRNA of circ_0003057 transfection. (d) Alkaline phosphatase and quantitative analysis after siRNA of circ_0003057 transfection. Scale bar: 1 mm. (e) Alizarin red and semi-quantitative analysis after siRNA of circ_0003057 transfection. Scale bar: 1 mm. (f) Plasmid transfection efficiency was detected by qRT-PCR after overexpression of circ_0003057. (g) qRT-PCR analysis the expression of ALP, OCN, RUNX-2, BSP, DSPP and DMP-1 after overexpression of circ_0003057. (h) Western blot and semi-quantitative analysis of DSPP, DMP-1 protein after overexpression of circ_0003057. (i) Alkaline phosphatase and quantitative analysis after overexpression of circ_0003057. Scale bar: 1 mm. (j) Alizarin red and semi-quantitative analysis after overexpression of circ_0003057. Scale bar: 1 mm. Quantitative data from three independent experiments are shown as the mean ± SD (error bars). $*p < 0.05$, $**p < 0.01$ and $***p < 0.001$. $n = 3$ biologically independent samples.

overexpression plasmid, we found that the mRNA expression levels of the relevant osteo-/odontogenic-associated genes ALP, RUNX-2, OCN, BSP, DSPP and DMP-1 increased accordingly (Figure 4b). Related osteo-/odontogenic genes were downregulated after decreasing ANKH expression (Figure 4d). Western blotting also showed the same trend, with increased expression levels of DSPP and DMP-1 in the OE -- ANKH group and decreased expression levels of DSPP and DMP-1 in the sh-ANKH group (Figure 4e,f). We found that with an upregulated expression level of ANKH in hDPSCs, ALP activity increased and the number of mineralized nodules stained with alizarin red increased (Figure 4g,h). Downregulation of ANKH expression showed the opposite trend (Figure 4i,j). These results suggest that ANKH may be involved in the osteo/odontogenic differentiation of hDPSCs.

Circ_0003057 through upregulated expression of ANKH promoted osteo/odontogenic differentiation of hDPSCs

To investigate the mechanistic relationship between circ_0003057 and its parental gene ANKH in the osteo/odontogenic differentiation of hDPSCs, we found that increasing and knocking down circ_0003057 expression and the mRNA and protein levels of ANKH after osteo/odontogenic induction culture of hDPSCs changed with circ_0003057 change (Figure 5a–d). Furthermore, in osteo/odontogenic differentiation cultures, changes in ANKH expression also caused changes in circ_0003057 expression (Figure 5e,f). Rescue experiments were performed to determine the upstream–downstream relationship between circ_0003057 and ANKH. The qRT-PCR assay revealed that overexpression of circ_0003057 resulted in upregulated expression levels of osteo/odontogenic genes, whereas lowering ANKH expression levels reversed the effect of circ_0003057 overexpression, resulting in a decrease in gene expression levels (Figure 5g). Western blot analysis confirmed this pattern, showing that decreased ANKH expression reduced the effect of circ_0003057 upregulation on osteo/odontogenic differentiation (Figure 5h). Collectively, these findings suggest that circ_0003057 facilitates the osteo/odontogenic differentiation of hDPSCs through the modulation of ANKH.

EIF4A3 binds to circ_0003057 and regulates osteo/odontogenic differentiation of hDPSCs

We excluded the possibility that circ_0003057 encodes proteins. The effect of RBPs drew our attention, and interaction with RBP is another important way for circRNAs to regulate downstream gene expression. The online databases CircInteractome (https://circinteractome.irp.nia.nih.gov/), CSCD (http://gb.whu.edu.cn/CSCD/) and RBP Suite (http://www.csbio.sjtu.edu.cn/bioinf/RBPsuite/) were used to screen the potential RBPs of circ_0003057 (Figure 6a). Predictions using an online database revealed that EIF4A3 with circ_0003057 had the highest number of binding sites. We found that hDPSCs underwent osteo/odontogenic differentiation, with increased levels of EIF4A3 mRNA expression, suggesting that EIF4A3 may be associated with osteo/odontogenic differentiation (Figure 6b). To verify the binding effect of EIF4A3 with circ_0003057, RNA immunoprecipitation (RIP) experiments further confirmed that the anti-EIF4A3 group showed more circ_0003057 binding to EIF4A3 than did the IgG group (Figure 6c). In addition, we performed RNA pull-down experiments and found that circ_0003057 was significantly enriched in the EIF4A3 protein compared to that in the control group (Figure 6d). Immunofluorescence/fish assays for subcellular co-localization showed a binding relationship between circ_0003057 and EIF4A3 in the cytoplasm (Figure 6e). We designed the siRNA and overexpression plasmids targeting EIF4A3 and successfully transfected them into hDPSCs. With high expression levels of EIF4A3, we detected the mRNA rise of the osteo/odontogenic markers RUNX-2, OCN, BSP, DSPP and DMP-1 (Figure 6f). Downregulation of EIF4A3 expression

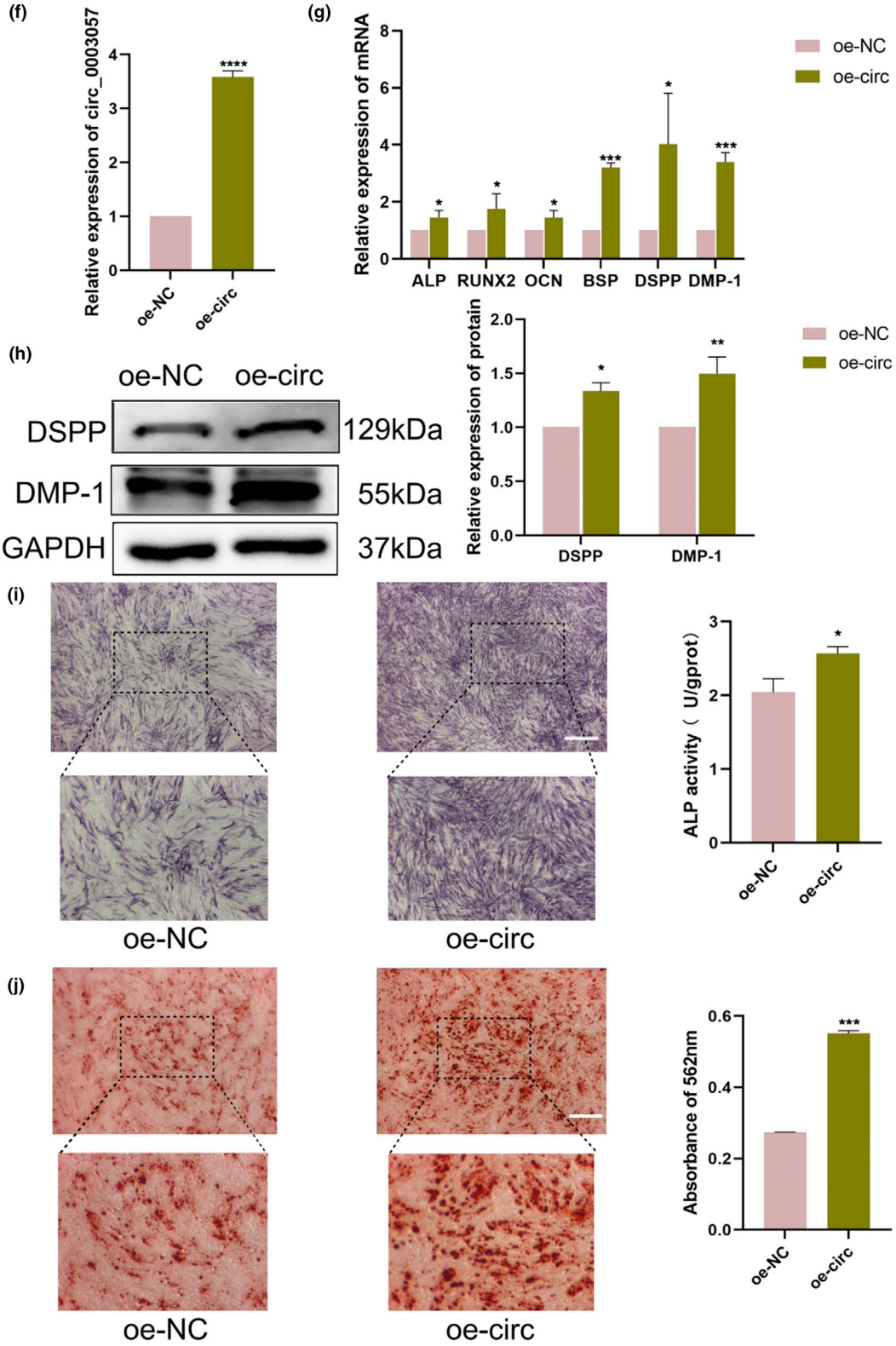

FIGURE 3 (Continued)

levels showed the reverse trend (Figure 6g). As the expression level of EIF4A3 increased, the western blot assay detected increased expression of DSPP and DMP-1 proteins in hDPSCs (Figure 6h). EIF4A3 knockdown resulted in decreased protein expression of DSPP and DMP-1 (Figure 6i). Simultaneously, ALP activity increased in hDPSCs with high EIF4A3 expression (Figure 6j). ALP activity was decreased after the knockdown of EIF4A3 (Figure 6k). These results suggested that EIF4A3 affects the osteo/odontogenic differentiation of hDPSCs.

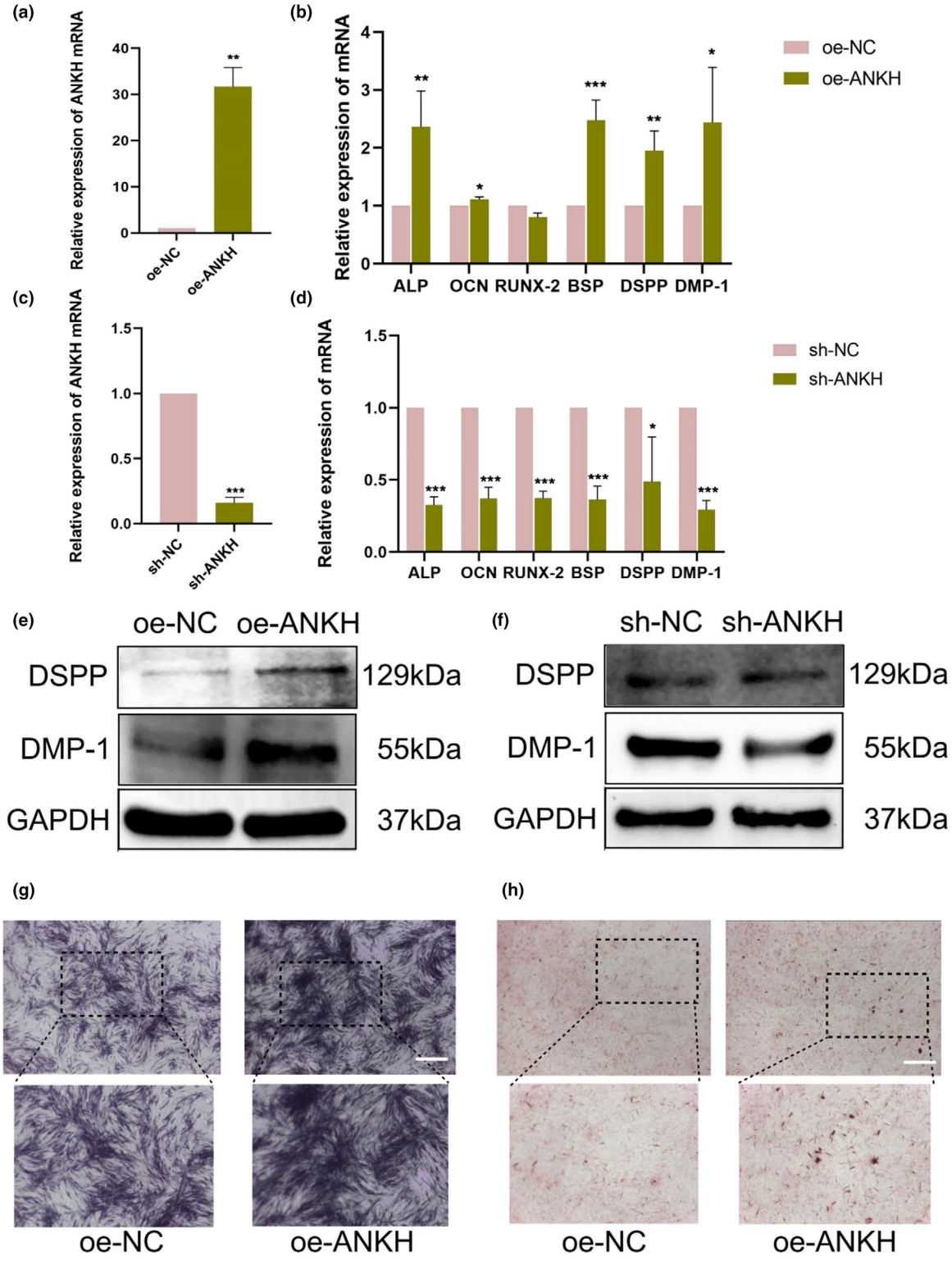

FIGURE 4 Upregulated expression of ANKH promotes osteo/odontogenic differentiation of hDPSCs. (a, c) Plasmid transfection efficiency was detected using qRT-PCR after transfection with interference expression and overexpression plasmids. (b, d) qRT-PCR analysis of the expression of ALP, OCN, RUNX-2, BSP, DSPP and DMP-1 after ANKH downregulated and upregulated expression. (e, f) Western blot and semi-quantitative analysis of DSPP, DMP-1 protein after downregulated expression and overexpression of ANKH. (g, i) Alkaline phosphatase and quantitative analysis after ANKH downregulated and upregulated expression. Scale bar: 1 mm. (h, j) Alizarin red and semi-quantitative analysis after ANKH downregulated and upregulated expression. Scale bar: 1 mm. Quantitative data from three independent experiments are shown as the mean ± SD (error bars). $^{*}p < 0.05$, $^{**}p < 0.01$ and $^{***}p < 0.001$. $n = 3$ biologically independent samples.

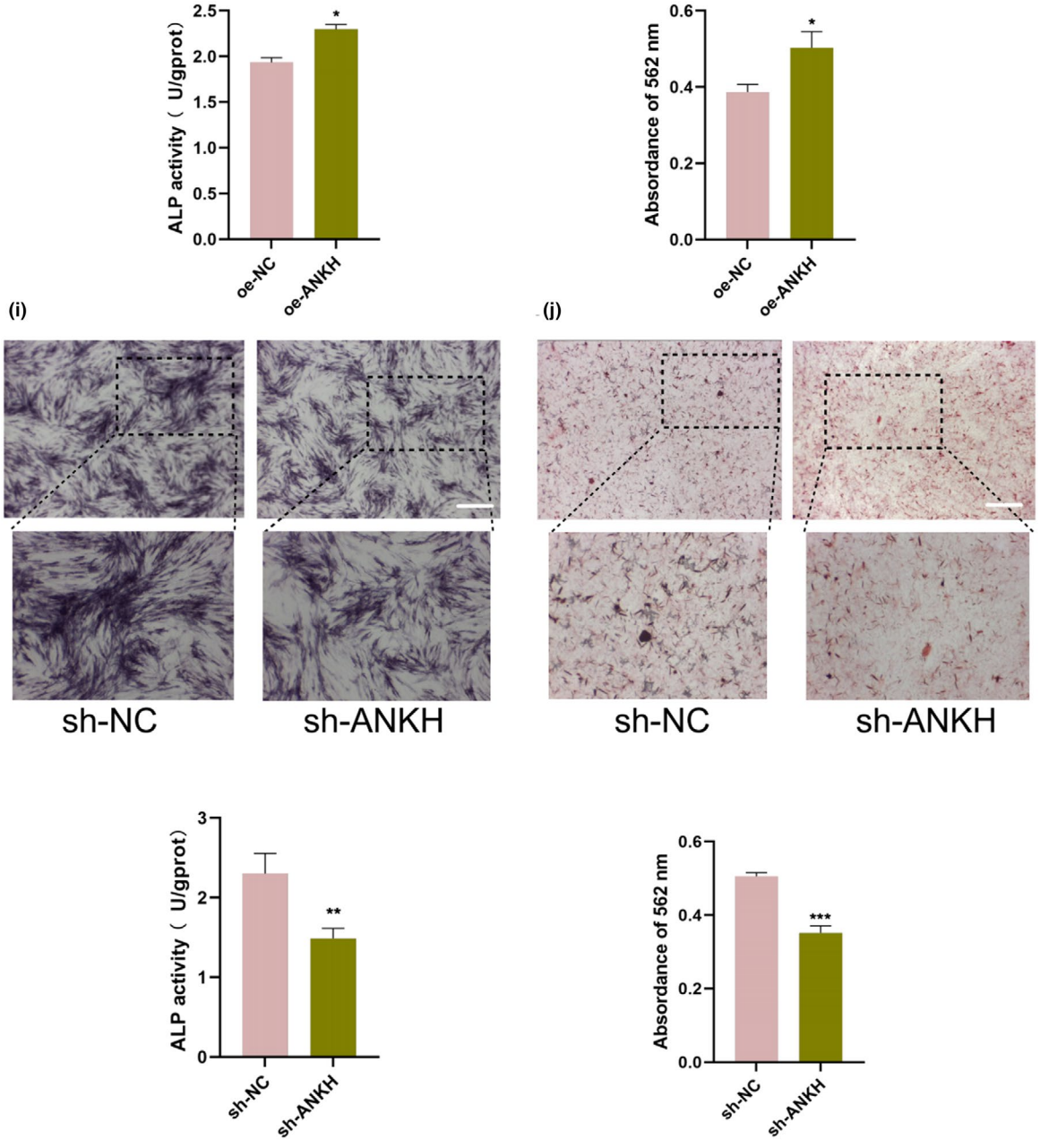

FIGURE 4 (Continued)

FIGURE 5 Circ_0003057 through upregulated expression of ANKH promoted osteo/odontogenic differentiation of hDPSCs (a, c) After knockdown expression of circ_0003057 and overexpression of circ_0003057 in osteo/odontogenic differentiation, ANKH was detected by qRT-PCR. (b, d) After knockdown expression of circ_0003057 and overexpression of circ_0003057 in osteo/odontogenic differentiation, the protein expression level of ANKH was detected and semi-quantitatively analysed using western blot. (e, f) circ_0003057 expression was detected using qRT-PCR after osteo/odontogenic differentiation of hDPSCs with knockdown expression of ANKH and overexpression of ANKH. (g) BSP, DSPP and DMP-1 mRNA expression levels in hDPSCs were detected using qRT-PCR after gene rescue experiments whereby circ_0003057 overexpression plasmid and ANKH interference plasmid were transfected with hDPSCs. (h) The DSPP and DMP-1 protein expression levels in hDPSCs were detected using western blotting after gene rescue experiments whereby circ_0003057 overexpression plasmid and ANKH interference plasmid were transfected with hDPSCs. Quantitative data from three independent experiments are shown as the mean ± SD (error bars). *$p < 0.05$, **$p < 0.01$ and ***$p < 0.001$. $n = 3$ biologically independent samples.

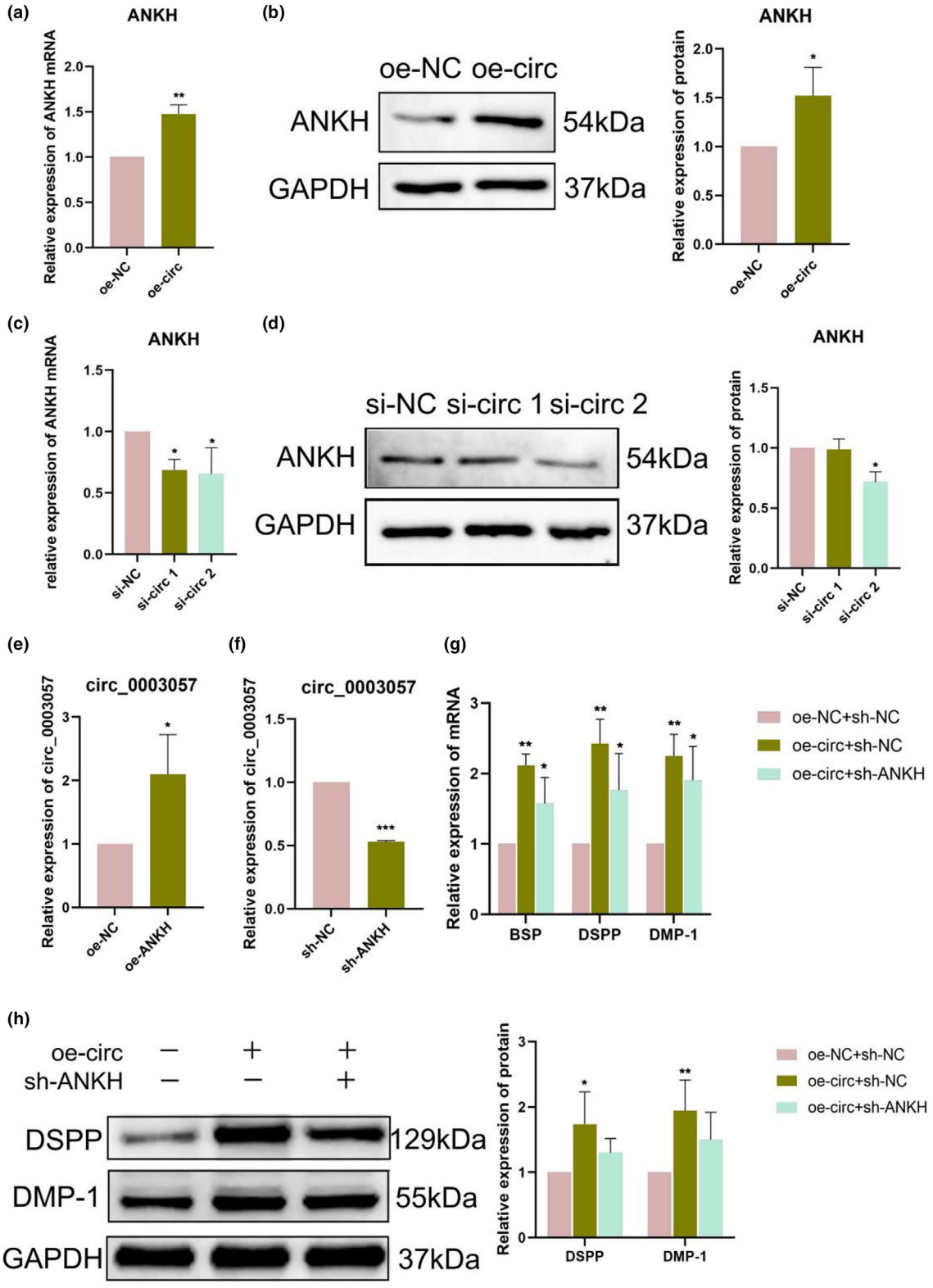

EIF4A3 affects the export of circ_0003057 from the nucleus to the cytoplasm

To explore the regulatory relationship between EIF4A3 and circ_0003057, we found that either an increase or decrease in circ_0003057 expression in hDPSCs caused changes in the expression levels of EIF4A3 mRNA and protein (Figure 7a–d). In contrast, downregulation of EIF4A3 expression reduced circ_0003057 expression (Figure 7e). EIF4A3 is a eukaryotic transcription factor that affects the transcription of multiple RNAs exported from the nucleus. Therefore, we extracted nucleoplasmic

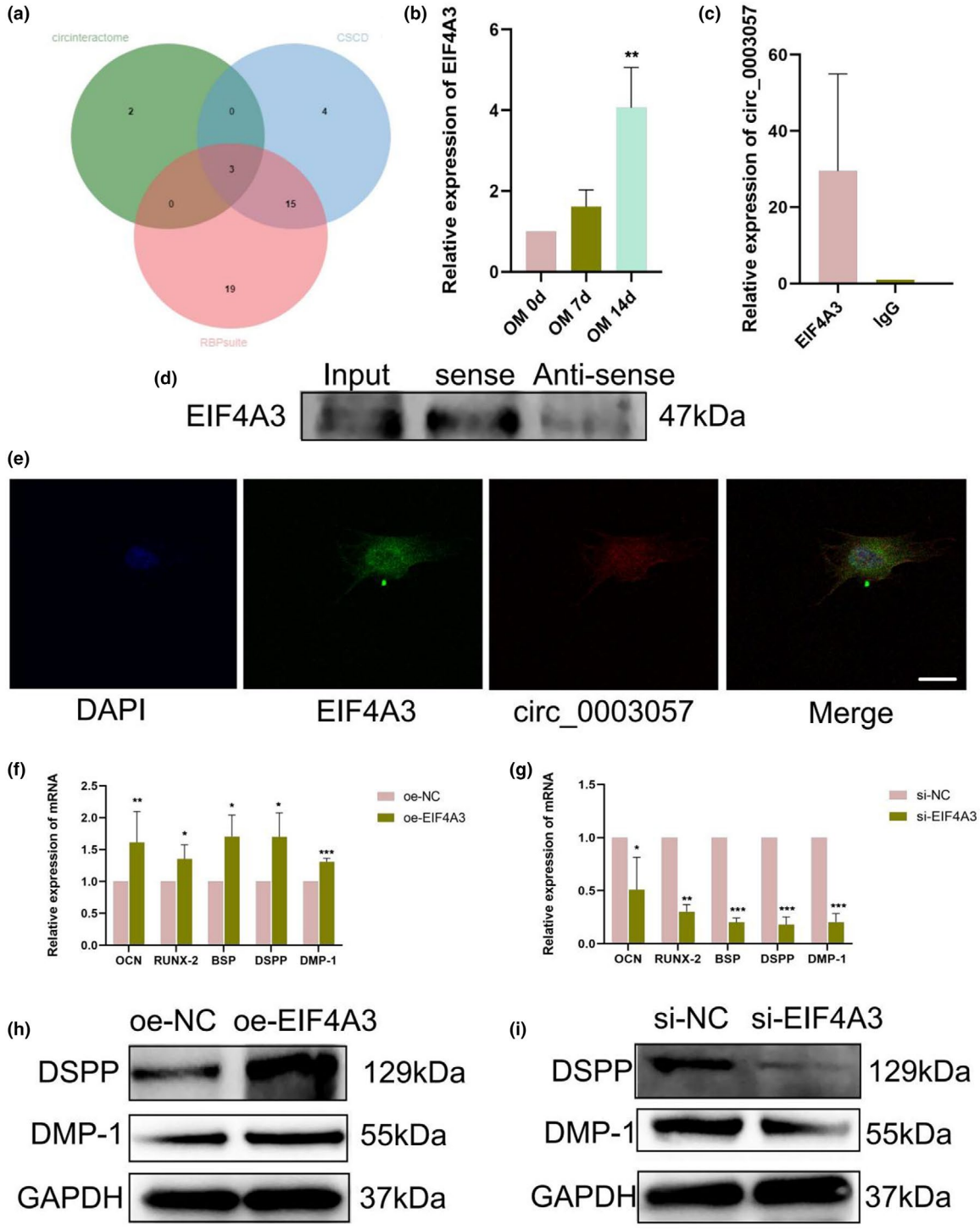

FIGURE 6 EIF4A3 binds to circ_0003057 and regulates osteo/odontogenic differentiation of hDPSCs. (a) Information website analyses were performed to identify candidate proteins that could interact with circ_0003057. (b) qRT-PCR was used to detect the expression level of EIF4A3 in hDPSC osteo/odontogenic differentiation at 0, 7 and 14 days of induction. (c) RIP assay using anti-EIF4A3 antibody was used to verify the binding of EIF4A3 to circ_0003057. (d) Western blot assay confirmed the interaction between EIF4A3 and circ_0003057 by RNA pull-down assay. (e) IF/FISH detection of circ_0003057 and EIF4A3 in hDPSC cells. Scale bar: 75 μm. (f, g) qRT-PCR was used to detect the mRNA expression levels of RUNX-2, BSP, DSPP and DMP-1 after downregulated and upregulated EIF4A3. (h, i) Western blot was used to detect the protein expression levels of DSPP and DMP-1 after downregulated and upregulated EIF4A3. (j, k) Alkaline phosphatase and quantitative analysis after downregulated and upregulated of EIF4A3. Scale bar: 1 mm. Quantitative data from three independent experiments are shown as the mean ± SD (error bars). $*p < 0.05$, $**p < 0.01$ and $***p < 0.001$. $n = 3$ biologically independent samples.

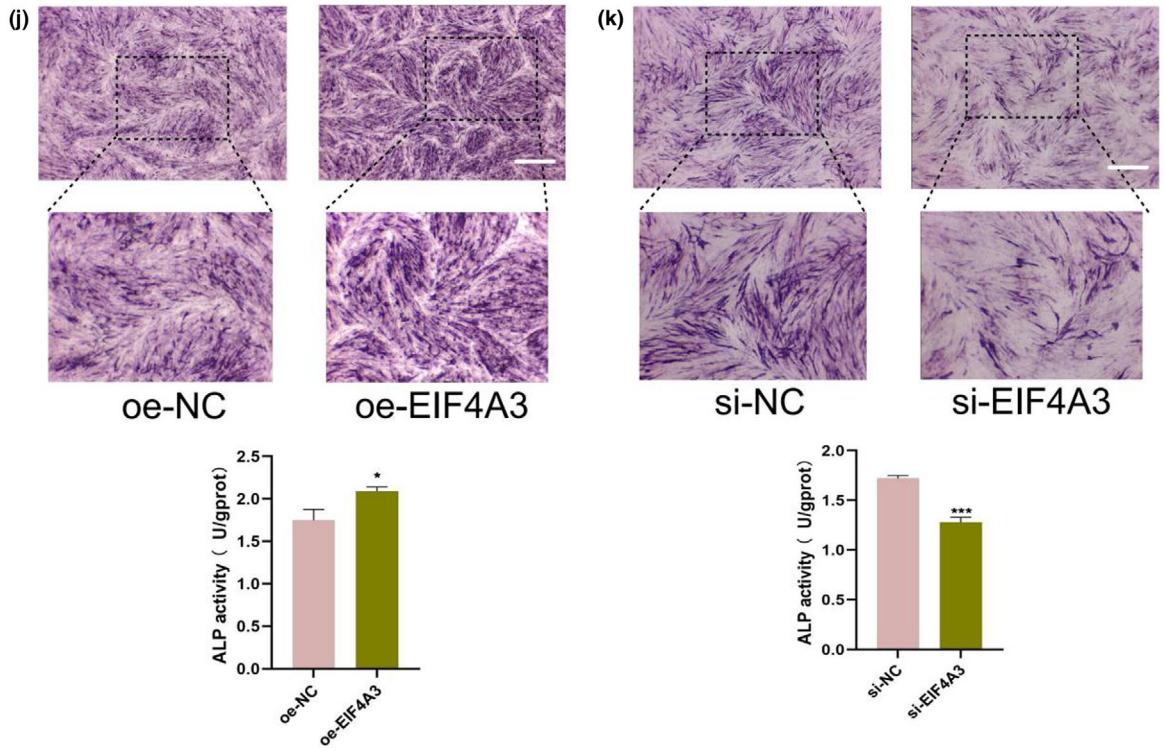

FIGURE 6 (Continued)

RNA from hDPSCs of knockdown EIF4A3 expression and found a decreased proportion of circ_0003057 in the cytoplasm (Figure 7f). We speculated that EIF4A3 might affect the osteo/odontogenic differentiation of hDPSCs by influencing the export of circ_0003057 from the nucleus.

Exosome circ_0003057 promotes osteo/odontogenic differentiation *in vivo*

To investigate the impact of exosomes with high levels of circ_0003057 on osteo/odontogenic differentiation in vivo, we prepared 3-mm-thick blocks of human dentine matrix. These blocks were injected into hydrogels containing hDPSCs co-cultured with exosomes. These blocks were then transplanted onto the backs of nude mice for 8 weeks (Figure 8a). We extracted pulp-like tissues formed within these blocks. qRT-PCR analysis revealed that the mRNA expression levels of RUNX-2, OCN, DSPP and DMP-1 were significantly elevated in the exosome group compared to those in the control, particularly in the EXO 7 group (Figure 8b). Haematoxylin and eosin (H&E) staining and Masson staining showed sparse cellular composition and a small amount of fibrous tissue in the blank control group. However, the hDPSCs group had a large number of spindle cells aggregated around the dentine block with some levels of fibrous tissue formation. The EXO 0d and EXO 7d groups formed dentine-like tissue around the dentine block, and there were a large number of spindle cells with some degree of aggregation around the dentine-like tissue, in which the dentine-like tissue in the EXO 7 group was thicker and denser (Figure 8c,d). These findings suggested that exosomes enriched with circ_0003057 significantly enhanced the development of dentine-like structures in vivo.

DISCUSSION

The DPC maintains the normal function and structural integrity of the entire tooth (Bjørndal et al., 2019). Initially, when the dental pulp is potentially inflamed, the goal of therapy is to maintain its vitality and regenerate the DPC to preserve the pulp and re-establish a protective mineralized barrier (Li et al., 2021). Regenerative endodontics uses the concept of tissue engineering to regenerate the DPC of immature permanent teeth with necrotic pulp due to infection, trauma, or developmental abnormalities (Kim et al., 2018). Stem cells and growth factors are the critical factors in the regeneration of dental pulp tissue engineering (Kim et al., 2018). hDPSCs, as the most common seed cells for tissue engineering pulp regeneration, have good self-expansion and multi-directional differentiation ability (Fawzy El-Sayed et al., 2019). Exosomes contain various biological factors that transmit cell-to-cell information and regulate cellular activity (Doyle & Wang, 2019).

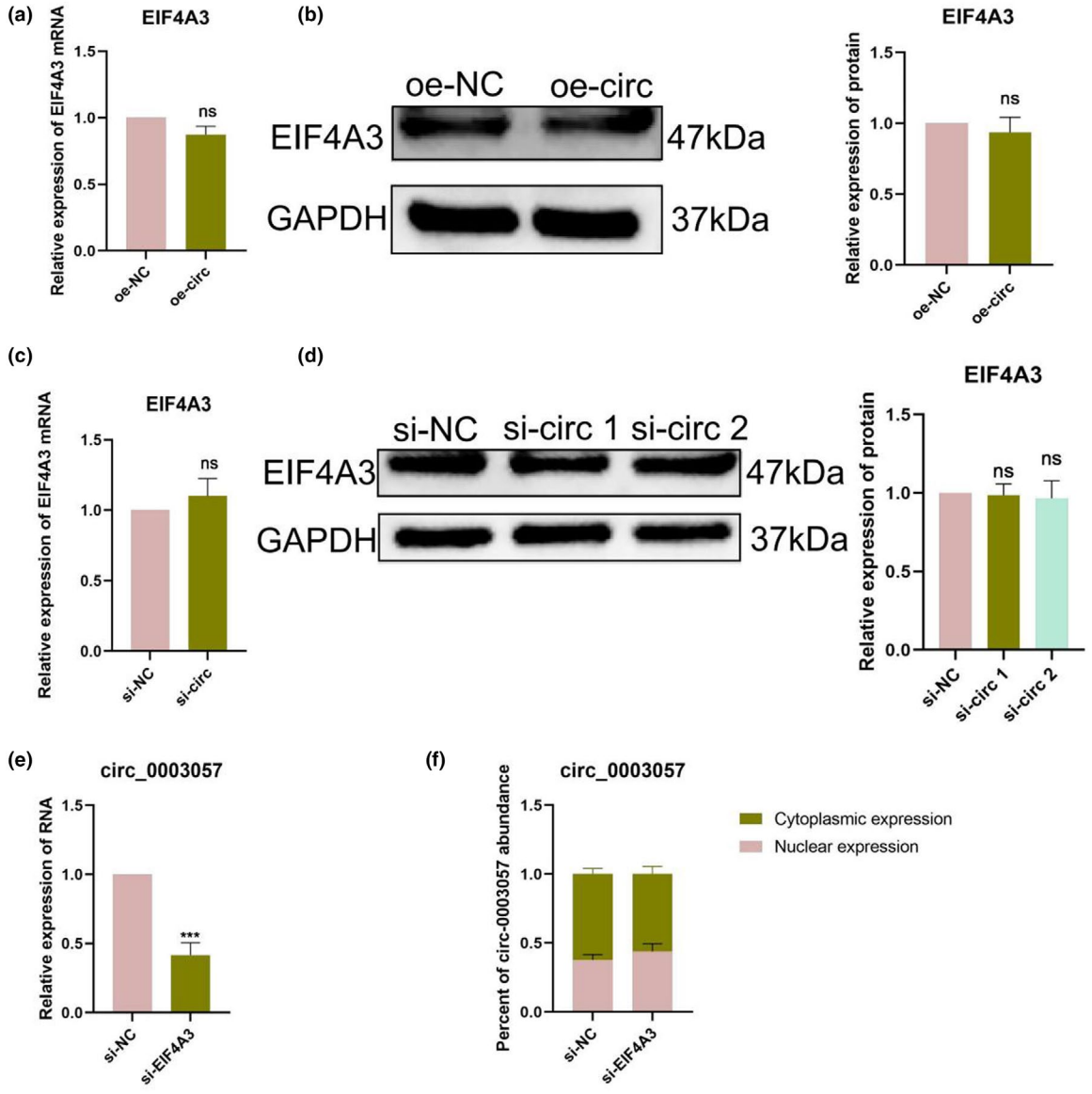

FIGURE 7 EIF4A3 affects the export of circ_0003057 from the nucleus to the cytoplasm. (a, c) EIF4A3 were detected by qRT-PCR after the knockdown expression of circ_0003057 and overexpression of circ_0003057 in hDPSCs. (b, d) EIF4A3 was detected and semi-quantitatively analysed using western blot after the knockdown expression of circ_0003057 and overexpression of circ_0003057 in hDPSCs. (e) Circ_0003057 in hDPSCs was detected using qRT-PCR after the knockdown expression of EIF4A3 in hDPSCs. (f) After the EIF4A3 interference plasmid was transferred into hDPSCs, the qRT-PCR assay detected the ratio of nuclear (Nuc) and cytoplasmic (Cyt) distribution of circ_0003057. Quantitative data from three independent experiments are shown as the mean ± SD (error bars). $*p < 0.05$, $**p < 0.01$ and $***p < 0.001$. $n = 3$ biologically independent samples.

Exploring the processes of exosome promoting hDPSCs osteo/odontogenic differentiation would thus aid in the advancement of this technology.

Exosomes can enhance mesenchymal cell proliferation and migration (Hammouda et al., 2023). For example, in vitro, exosomes derived from hDPSCs triggered the P38 MAPK pathway and increased the expression of genes for osteo/odontogenic differentiation of hDPSCs and hBMSCs (Huang et al., 2016). They upregulated osteo/odontogenic gene expression involving BSP, DSPP and VEGF and consequently improved the mineralization activity of hDPSCs (Swanson et al., 2020). In vivo and in vitro studies, we found that extracting exosomes from day 7 of mineralization-induced culture improved the osteo/odontogenic differentiation of hDPSCs. A study found that exosomes isolated under mineralized conditions induced greater hDPSC differentiation than exosomes isolated under conventional conditions using exosomal miR-27a-5p (Hu et al., 2019). Likewise, exosomes trigger the regeneration of dentine pulp-like

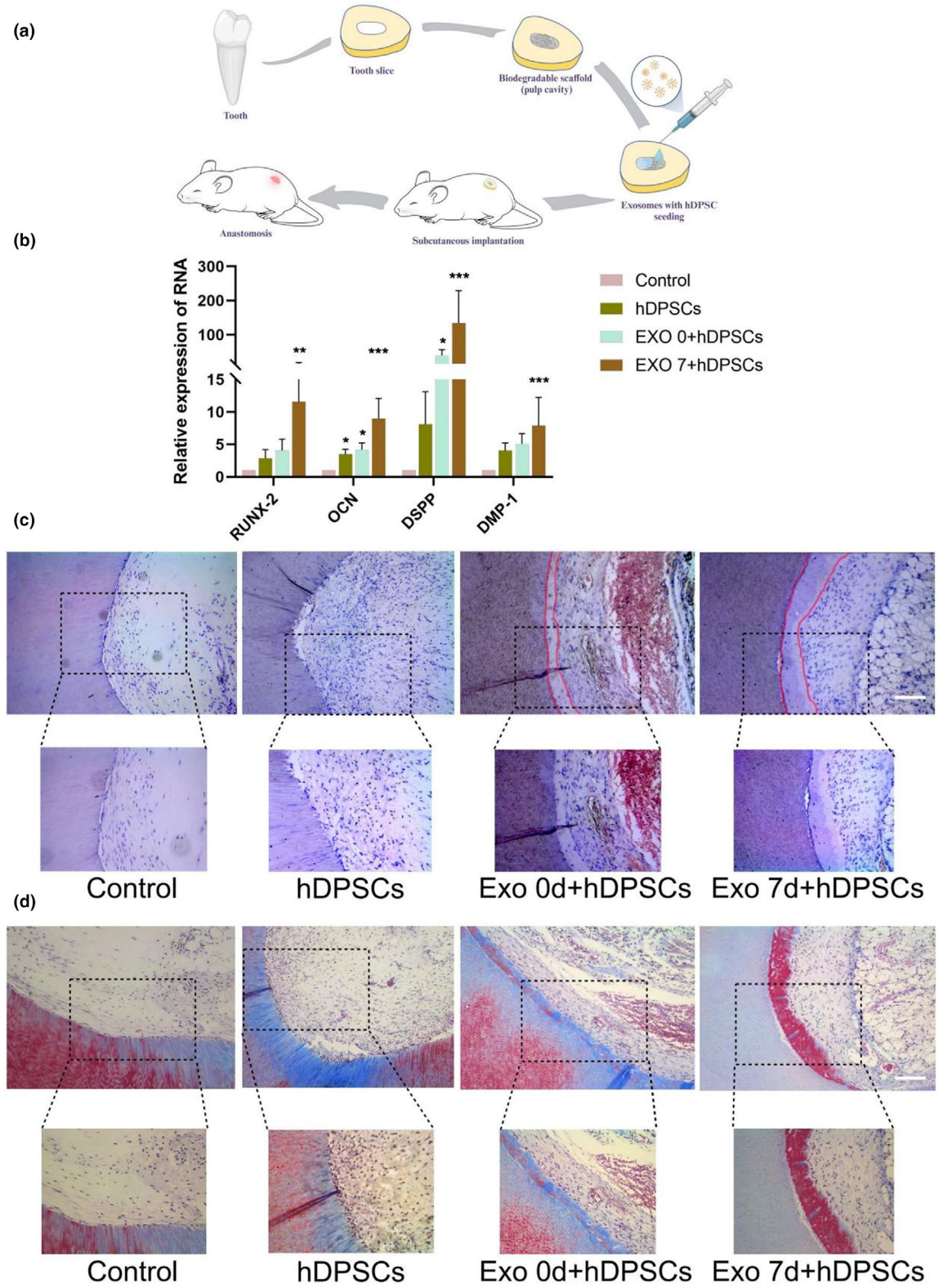

FIGURE 8 Exosome circ_0003057 promotes osteo/odontogenic differentiation in vivo. (a) Schematic illustration of the experimental animal setup. (b) Dentine blocks loaded with exosomes and hDPSCs were implanted onto the backs of nude mice for 8 weeks. RNA was subsequently extracted from these tissues, and mRNA levels of RUNX-2, OCN, DSPP and DMP-1 were quantified using qRT-PCR. (c) H&E staining of tissue sections from the transplanted dentine blocks. Scale bar: 200 μm. (d) Masson's trichrome staining of tissue sections from the transplanted dentine blocks. Scale bar: 200 μm. Dentine-like tissue regions are indicated by circles. Quantitative data from three independent experiments are shown as the mean ± SD (error bars). $*p < 0.05$, $**p < 0.01$ and $***p < 0.001$. $n = 6$ biologically independent samples.

tissues, and exosomes isolated under odontogenic conditions are better inducers of odontogenic differentiation and tissue regeneration than those isolated under growth conditions (Huang et al., 2016). Our study found that hDPSCs-derived exosome circ_0003057 was significantly elevated on the seventh day of osteo/odontogenic differentiation and that this exosome was the most effective in promoting differentiation. This suggests that exosomal circ_0003057 plays an important role in osteo/odontogenic differentiation.

Some recent studies linked circRNAs to the osteo/odontogenic differentiation of dental tissue-derived MSCs. For example, circIGSF11 silencing increases miR-199b-5p expression and enhances osteoblast differentiation (Zhang et al., 2019). Circ_0026827 promotes osteo/odontogenic differentiation of DPSCs via Beclin1 and the RUNX1 signalling pathways by sponging miR-188-3p (Ji et al., 2020). In the current study, we found that circ_0003057 expression in hDPSCs significantly increased during osteo/odontogenic differentiation. Circ_0003057 was mainly located in the cytoplasm of hDPSCs. According to the analysis of databases such as circBase, circBank and NCBI, circ_0003057 is formed by the 3′-8′ splice site of the mRNA exon 3′-8′ of ANKH originating from the gene located on chr5:14741935–14 758 707, and its length is 698 nt. Downregulation of circ_0003057 suppresses osteo/odontogenic differentiation, whereas elevated expression of circ_0003057 promotes osteo/odontogenic differentiation. We speculated that hDPSCs could take up exosomes normally and that exosomes could piggyback on circ_0003057 delivered to hDPSCs, thereby promoting osteo/odontogenic differentiation.

There is evidence that the parental genes of circRNAs are also involved in circRNA function (Wan et al., 2016). Circ_0003057 of parental genes, ANKH, played various roles in regulating cellular events surrounding differentiation and mineralization in bone and cartilage (Williams, 2016). Progressive ankylosis (ANK) has been suggested to function as a multipass transmembrane protein with similarities to known transporters, and the human homologue of the ANK gene is termed ANKH (Williams, 2016). Previous studies have shown that ANK deficiency suppresses the osteoblast differentiation of BMSCs from ank/ank mice (Kim et al., 2010). ANK is a regulator of both osteoblastic and osteoclastic differentiation events (Williams, 2016). During the osteo/odontogenic differentiation of hDPSCs, we found that circ_0003057 has a regulatory effect on ANKH and affects the level of ANKH expression, which in turn affects the expression of circ_0003057. These studies indicate that circ_0003057 exerts its function through ANKH. We performed rescue experiments and found that downregulated expression of ANKH can reverse the overexpression of circ_0003057 to suppress osteo/odontogenic differentiation. We believe that since an increase in circ_0003057 causes an increase in the expression of ANKH, and an increase in ANKH causes an increase in the cyclization of circ_0003057, circ_0003057 can play a role in influencing the osteo/odontogenic differentiation of hDPSCs through the regulation of ANKH.

Recent studies have reported that circRNAs play crucial roles in regulating gene expression at the transcriptional level by interacting with RBPs (Li et al., 2015). CircPOK was found to bind the RNA/DNA-binding proteins ILF2 and ILF3 mainly in the nucleus and potentiate their regulatory activities in mediating both mRNA transcription and stability (Guarnerio et al., 2019). Through bioinformatics prediction, we identified EIF4A3 as a possible circ_0003057 binding protein and successfully verified their binding roles using RNA pull-down experiments and RIP experiments. Previous studies have shown that EIF4A3 promotes the expression of most circRNAs (Zhang et al., 2020). Previous research showed that circRNA-binding proteins play critical roles in regulating circRNA synthesis and degradation (Conn et al., 2015). EIF4A3 plays essential roles in mRNA splicing, nuclear mRNA export, subcellular mRNA localization, translation efficiency and nonsense-mediated mRNA decay (Giorgi et al., 2007). EIF4A3, a eukaryotic initiation factor, promotes increased circ_0042881 cyclization and promotes breast cancer progression (Ju et al., 2023). By reducing the expression of EIF4A3, we found that the mRNA expression levels of osteo/odontogenic markers decreased, as did the expression of circ_0003057. Our study revealed that EIF4A3 might act as an activator of circ_0003057 and regulate its expression. We isolated RNA from the nucleus and cytoplasm of hDPSCs and found that the expression level of circ_0003057 decreased proportionally in the cytoplasm after EIF4A3 was downregulated. A previous study has shown that circSEMA5A influences the stability of the parental gene SEMA5A by recruiting EIF4A3, which in turn increases the expression of SEMA5A, thereby promoting angiogenesis (Wang et al., 2020). As EIF4A3 is a known mediator of nuclear RNA export, its binding to circ_0003057 may facilitate the cytoplasmic accumulation of circRNAs, thereby enhancing ANKH translation. Collectively, we speculated that EIF4A3 may promote the release of circ_0003057 out of the nucleus, and that the high expression of circ_0003057 stimulates the upregulation of ANKH mRNA expression, subsequently improving the osteo/odontogenic differentiation of hDPSCs (Figure 9). These findings may provide new insights into the potential role of exosomes in the treatment of reconstructive REPs. Whilst our study demonstrates the exosomal circ_0003057-EIF4A3-ANKH axis, the upstream

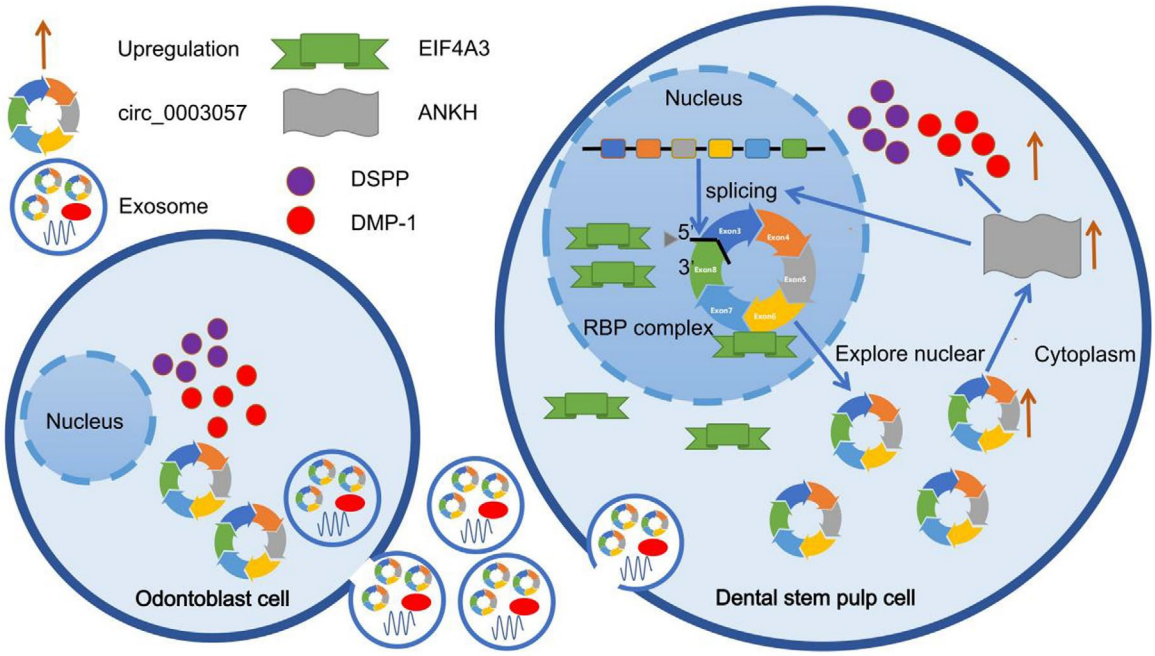

FIGURE 9 Schematic illustration indicates the mechanism of exosomal circ_0003057 promoting the osteo/odontogenic differentiation of hDPSCs by interacting with EIF4A3 through parental gene ANKH mRNA upregulation.

signals regulating circ_0003057 biogenesis during differentiation remain unclear. Future studies should explore the transcriptional regulators of ANKH splicing.

Although this study reveals the mechanism by which exosome circ_0003057 regulates the differentiation of hDPSCs through the EIF4A3-ANKH axis, limitations remain. For example, the impact of exosome heterogeneity on function has not been systematically assessed, and clinical translation requires further validation of its long-term safety and targeted delivery efficiency. Future studies could incorporate multi-omics techniques to analyse the dynamic profile of exosomal circRNAs and develop engineered exosomes to optimize regenerative efficacy and promote their clinical application in endodontic regeneration.

CONCLUSIONS

circ_0003057 was upregulated during osteo/odontogenic differentiation of hDPSCs, and exosomes with high circ_0003057 expression significantly promoted osteo/odontogenic differentiation. Mechanistically, EIF4A3 binds to circ_0003057, promotes circ_0003057 release from the nucleus and upregulates ANKH expression, thereby promoting osteo/odontogenic differentiation of hDPSCs. Targeted exosomal circ_0003057 delivery may represent a novel strategy for DPC regeneration in clinical endodontics.

AUTHOR CONTRIBUTIONS

BingtaoWang, Yuanyuan Kong and Qianzhou Jiang initiated and designed the study. Bingtao Wang, Huixian Dong, Feng Lai, Zixin Guo, Liecong Lin, Jingyi Xu and Jingkun Zhang conducted the experiments. BingtaoWang performed data analysis. Yiguo Jiang, Qianzhou Jiang provided administrative, technical or material support. BingtaoWang, Yuanyuan Kong and Qianzhou Jiang completed manuscript writing, review and/or revision. Yuanyuan Kong and Qianzhou Jiang performed supervision of the study. Yuanyuan Kong and Qianzhou Jiang provided funding acquisition.

All authors gave their final approval and agreed to be accountable for all aspects of the work.

FUNDING INFORMATION

This study was supported by the National Natural Science Foundation of China (82270966), Natural Science Foundation of Guangdong Province (2024A1515012741) and Guangdong Basic and Applied Basic Research Foundation Project (2022A1515110601).

CONFLICT OF INTEREST STATEMENT

The authors declare no conflict of interest.

DATA AVAILABILITY STATEMENT

The data that support the findings of this study are available from the corresponding author upon reasonable request.

ETHICS STATEMENT

The Ethics Committee of the Hospital of Stomatology of Guangzhou Medical University gave clearance to this study (No. JCYJ2024029). The animal experiment was conducted in accordance with the animal care guidelines approved by Ruiye Bio-tech Guangzhou Co. Ltd. Experimental Animal Ethics Committee (No. RYEth-20 240 412 429).

ORCID

Qianzhou Jiang https://orcid.org/0000-0003-2631-7527

REFERENCES

Abdelmohsen, K., Panda, A.C., Munk, R., Grammatikakis, I., Dudekula, D.B., de, S. et al. (2017) Identification of HuR target circular RNAs uncovers suppression of PABPN1 translation by CircPABPN1. *RNA Biology*, 14(3), 361–369.

Ashwal-Fluss, R., Meyer, M., Pamudurti, N.R., Ivanov, A., Bartok, O., Hanan, M. et al. (2014) circRNA biogenesis competes with pre-mRNA splicing. *Molecular Cell*, 56(1), 55–66.

Batouli, S., Miura, M., Brahim, J., Tsutsui, T.W., Fisher, L.W., Gronthos, S. et al. (2003) Comparison of stem-cell-mediated osteogenesis and dentinogenesis. *Journal of Dental Research*, 82(12), 976–981.

Bjørndal, L., Simon, S., Tomson, P.L. & Duncan, H.F. (2019) Management of deep caries and the exposed pulp. *International Endodontic Journal*, 52(7), 949–973.

Chen, G., Shi, Y., Zhang, Y. & Sun, J. (2017) CircRNA_100782 regulates pancreatic carcinoma proliferation through the IL6-STAT3 pathway. *Oncotargets and Therapy*, 10, 5783–5794.

Conn, S.J., Pillman, K.A., Toubia, J., Conn, V.M., Salmanidis, M., Phillips, C.A. et al. (2015) The RNA binding protein quaking regulates formation of circRNAs. *Cell*, 160(6), 1125–1134.

Deng, J., Pan, T., Lv, C., Cao, L., Li, L., Zhou, X. et al. (2023) Exosomal transfer leads to chemoresistance through oxidative phosphorylation-mediated stemness phenotype in colorectal cancer. *Theranostics*, 13(14), 5057–5074.

Doyle, L.M. & Wang, M.Z. (2019) Overview of extracellular vesicles, their origin, composition, purpose, and methods for exosome isolation and analysis. *Cells*, 8(7), 727.

Fawzy El-Sayed, K.M., Elsalawy, R., Ibrahim, N., Gadalla, M., Albargasy, H., Zahra, N. et al. (2019) The dental pulp stem/progenitor cells-mediated inflammatory-regenerative Axis. *Tissue Engineering. Part B, Reviews*, 25(5), 445–460.

Giorgi, C., Yeo, G.W., Stone, M.E., Katz, D.B., Burge, C., Turrigiano, G. et al. (2007) The EJC factor eIF4AIII modulates synaptic strength and neuronal protein expression. *Cell*, 130(1), 179–191.

Guarnerio, J., Zhang, Y., Cheloni, G., Panella, R., Mae Katon, J., Simpson, M. et al. (2019) Intragenic antagonistic roles of protein and circRNA in tumorigenesis. *Cell Research*, 29(8), 628–640.

Hammouda, D.A., Mansour, A.M., Saeed, M.A., Zaher, A.R. & Grawish, M.E. (2023) Stem cell-derived exosomes for dentin-pulp complex regeneration: a mini-review. *Restorative Dentistry & Endodontics*, 48(2), e20.

Hansen, T.B., Jensen, T.I., Clausen, B.H., Bramsen, J.B., Finsen, B., Damgaard, C.K. et al. (2013) Natural RNA circles function as efficient microRNA sponges. *Nature*, 495(7441), 384–388.

Hentze, M.W. & Preiss, T. (2013) Circular RNAs: splicing's enigma variations. *The EMBO Journal*, 32(7), 923–925.

Høiby, N., Ciofu, O., Johansen, H.K., Song, Z.J., Moser, C., Jensen, P.Ø. et al. (2011) The clinical impact of bacterial biofilms. *International Journal of Oral Science*, 3(2), 55–65.

Hu, X., Zhong, Y., Kong, Y., Chen, Y., Feng, J. & Zheng, J. (2019) Lineage-specific exosomes promote the odontogenic differentiation of human dental pulp stem cells (DPSCs) through TGFbeta1/smads signaling pathway via transfer of microRNAs. *Stem Cell Research & Therapy*, 10(1), 170.

Huang, A., Zheng, H., Wu, Z., Chen, M. & Huang, Y. (2020) Circular RNA-protein interactions: functions, mechanisms, and identification. *Theranostics*, 10(8), 3503–3517.

Huang, C.C., Narayanan, R., Alapati, S. & Ravindran, S. (2016) Exosomes as biomimetic tools for stem cell differentiation: applications in dental pulp tissue regeneration. *Biomaterials*, 111, 103–115.

Huang, G.T., Gronthos, S. & Shi, S. (2009) Mesenchymal stem cells derived from dental tissues vs. those from other sources: their biology and role in regenerative medicine. *Journal of Dental Research*, 88(9), 792–806.

Ji, F., Zhu, L., Pan, J., Shen, Z., Yang, Z., Wang, J. et al. (2020) hsa_circ_0026827 promotes osteoblast differentiation of human dental pulp stem cells through the Beclin1 and RUNX1 signaling pathways by sponging miR-188-3p. *Frontiers in Cell and Development Biology*, 8, 470.

Ju, C., Zhou, M., Du, D., Wang, C., Yao, J., Li, H. et al. (2023) EIF4A3-mediated circ_0042881 activates the RAS pathway via miR-217/SOS1 axis to facilitate breast cancer progression. *Cell Death & Disease*, 14(8), 559.

Kim, H.J., Minashima, T., McCarthy, E.F., Winkles, J.A. & Kirsch, T. (2010) Progressive ankylosis protein (ANK) in osteoblasts and osteoclasts controls bone formation and bone remodeling. *Journal of Bone and Mineral Research*, 25(8), 1771–1783.

Kim, S.G., Malek, M., Sigurdsson, A., Lin, L.M. & Kahler, B. (2018) Regenerative endodontics: a comprehensive review. *International Endodontic Journal*, 51(12), 1367–1388.

Kristensen, L.S., Andersen, M.S., Stagsted, L.V.W., Ebbesen, K.K., Hansen, T.B. & Kjems, J. (2019) The biogenesis, biology and characterization of circular RNAs. *Nature Reviews. Genetics*, 20(11), 675–691.

Li, J., Rao, Z., Zhao, Y., Xu, Y., Chen, L., Shen, Z. et al. (2020) A decellularized matrix hydrogel derived from human dental pulp promotes dental pulp stem cell proliferation, migration, and induced multidirectional differentiation in vitro. *Journal of Endodontics*, 46(10), 1438–1447.e1435.

Li, S., Li, Y., Chen, B., Zhao, J., Yu, S., Tang, Y. et al. (2018) exoRBase: a database of circRNA, lncRNA and mRNA in human blood exosomes. *Nucleic Acids Research*, 46(D1), D106–d112.

Li, X., Zheng, Y., Zheng, Y., Huang, Y., Zhang, Y., Jia, L. et al. (2018) Circular RNA CDR1as regulates osteoblastic differentiation of periodontal ligament stem cells via the miR-7/GDF5/SMAD and p38 MAPK signaling pathway. *Stem Cell Research & Therapy*, 9(1), 232.

Li, Z., Huang, C., Bao, C., Chen, L., Lin, M., Wang, X. et al. (2015) Exon-intron circular RNAs regulate transcription in the nucleus. *Nature Structural & Molecular Biology*, 22(3), 256–264.

Li, Z., Liu, L., Wang, L. & Song, D. (2021) The effects and potential applications of concentrated growth factor in dentin-pulp complex regeneration. *Stem Cell Research & Therapy*, 12(1), 357.

Liu, J., Jin, T., Chang, S., Ritchie, H.H., Smith, A.J. & Clarkson, B.H. (2007) Matrix and TGF-beta-related gene expression during human dental pulp stem cell (DPSC) mineralization. *In Vitro Cellular & Developmental Biology. Animal*, 43(3–4), 120–128.

Liu, J., Liu, T., Wang, X. & He, A. (2017) Circles reshaping the RNA world: from waste to treasure. *Molecular Cancer*, 16(1), 58.

Liu, T., Zhang, X., Du, L., Wang, Y., Liu, X., Tian, H. et al. (2019) Exosome-transmitted miR-128-3p increase chemosensitivity of oxaliplatin-resistant colorectal cancer. *Molecular Cancer*, 18(1), 43.

Liu, Z., Li, S., Xu, S., A Bu du Xi Ku, N.E.B.Y., Wen, J., Zeng, X. et al. (2023) Hsa_Circ_0005044 promotes osteo/odontogenic differentiation of dental pulp stem cell via modulating miR-296-3p/FOSL1. *DNA and Cell Biology*, 42(1), 14–26.

Nagendrababu, V., Murray, P.E., Ordinola-Zapata, R., Peters, O.A., Rôças, I.N., Siqueira, J.F., Jr. et al. (2021) PRILE 2021 guidelines for reporting laboratory studies in endodontology: explanation and elaboration. *International Endodontic Journal*, 54(9), 1491–1515.

Nawaz, M., Shah, N., Zanetti, B.R., Maugeri, M., Silvestre, R.N., Fatima, F. et al. (2018) Extracellular vesicles and matrix remodeling enzymes: the emerging roles in extracellular matrix remodeling, progression of diseases and tissue repair. *Cells*, 7(10), 167.

Nuti, N., Corallo, C., Chan, B.M., Ferrari, M. & Gerami-Naini, B. (2016) Multipotent differentiation of human dental pulp stem cells: a literature review. *Stem Cell Reviews and Reports*, 12(5), 511–523.

Panda, A.C. (2018) Circular RNAs act as miRNA sponges. *Advances in Experimental Medicine and Biology*, 1087, 67–79.

Qu, L., Ding, J., Chen, C., Wu, Z.J., Liu, B., Gao, Y. et al. (2016) Exosome-transmitted lncARSR promotes sunitinib resistance in renal cancer by acting as a competing endogenous RNA. *Cancer Cell*, 29(5), 653–668.

Shen, Z., Kuang, S., Zhang, Y., Yang, M., Qin, W., Shi, X. et al. (2020) Chitosan hydrogel incorporated with dental pulp stem cell-derived exosomes alleviates periodontitis in mice via a macrophage-dependent mechanism. *Bioactive Materials*, 5(4), 1113–1126.

Swanson, W.B., Gong, T., Zhang, Z., Eberle, M., Niemann, D., Dong, R. et al. (2020) Controlled release of odontogenic exosomes from a biodegradable vehicle mediates dentinogenesis as a novel biomimetic pulp capping therapy. *Journal of Controlled Release*, 324, 679–694.

Tye, C.E., Gordon, J.A., Martin-Buley, L.A., Stein, J.L., Lian, J.B. & Stein, G.S. (2015) Could lncRNAs be the missing links in control of mesenchymal stem cell differentiation? *Journal of Cellular Physiology*, 230(3), 526–534.

Villani, C., Murugan, P. & George, A. (2024) Exosome-laden hydrogels as promising carriers for Oral and bone tissue engineering: insight into cell-free drug delivery. *International Journal of Molecular Sciences*, 25(20), 11092.

Wan, L., Zhang, L., Fan, K., Cheng, Z.-X., Sun, Q.-C. & Wang, J.-J. (2016) Circular RNA-ITCH suppresses lung cancer proliferation via inhibiting the Wnt/β-catenin pathway. *BioMed Research International*, 2016, 1–11.

Wang, L., Li, H., Qiao, Q., Ge, Y., Ma, L. & Wang, Q. (2020) Circular RNA circSEMA5A promotes bladder cancer progression by upregulating ENO1 and SEMA5A expression. *Aging (Albany NY)*, 12(21), 21674–21686.

Williams, C.J. (2016) The role of ANKH in pathologic mineralization of cartilage. *Current Opinion in Rheumatology*, 28(2), 145–151.

Zhang, C., Han, X., Yang, L., Fu, J., Sun, C., Huang, S. et al. (2020) Circular RNA circPPM1F modulates M1 macrophage activation and pancreatic islet inflammation in type 1 diabetes mellitus. *Theranostics*, 10(24), 10908–10924.

Zhang, M., Jia, L. & Zheng, Y. (2019) circRNA expression profiles in human bone marrow stem cells undergoing osteoblast differentiation. *Stem Cell Reviews and Reports*, 15(1), 126–138.

Zheng, X., Chen, L., Zhou, Y., Wang, Q., Zheng, Z., Xu, B. et al. (2019) A novel protein encoded by a circular RNA circPPP1R12A promotes tumor pathogenesis and metastasis of colon cancer via hippo-YAP signaling. *Molecular Cancer*, 18(1), 47.

SUPPORTING INFORMATION

Additional supporting information can be found online in the Supporting Information section at the end of this article.

How to cite this article: Wang, B., Kong, Y., Dong, H., Lai, F., Guo, Z., Lin, L. et al. (2025) Exosomal circ_0003057 promotes osteo/odontogenic differentiation of hDPSCs by binding with EIF4A3 through upregulated parental gene ANKH. *International Endodontic Journal*, 00, 1–23. Available from: https://doi.org/10.1111/iej.14262